UNIVERSITY OF MALTA
Faculty of Science
Department of Geosciences

DISSERTATION
M.Sc. in Applied Oceanography
Study Unit GSC5512

Applying CMEMS Ocean Model Data to Monitor Seasonal Variability of Temperature and Salinity Profiles in the Central Mediterranean Sea

by

Laura Holleran

Supervised by Dr. Anthony Galea

A dissertation submitted in partial fulfilment
of the requirements of the award of
Master of Science in Applied Oceanography of the University of Malta

L-Università ta' Malta

FACULTY/INSTITUTE/CENTRE/SCHOOL UM Faculty of Science

DECLARATIONS BY POSTGRADUATE STUDENTS

Student's Code [redacted]

Student's Name & Surname Laura Holleran

Course GSC5512

Title of Dissertation
Applying CMEMS Ocean Model Data to Monitor Seasonal Variability of Temperature and Salinity Profiles in the Central Medtierranean Sea

(a) Authenticity of Dissertation

I hereby declare that I am the legitimate author of this Dissertation and that it is my original work.

No portion of this work has been submitted in support of an application for another degree or qualification of this or any other university or institution of higher education.

I hold the University of Malta harmless against any third party claims with regard to copyright violation, breach of confidentiality, defamation and any other third party right infringement.

(b) Research Code of Practice and Ethics Review Procedures

I declare that I have abided by the University's Research Ethics Review Procedures. Research Ethics & Data Protection form code SCI-2024-00136.

As a Master's student, as per Regulation 77 of the General Regulations for University Postgraduate Awards 2021, I accept that should my dissertation be awarded a Grade A, it will be made publicly available on the University of Malta Institutional Repository.

[redacted]
Signature of Student

LAURA HOLLERAN
Name of Student (in Caps)

11/11/2024
Date

Acknowledgements

This dissertation was completed with the support of Dr. Anthony Galea as supervisor and with the use of data provided by the E.U. Copernicus Marine Service.

Abstract

Stratification of the Mediterranean Sea can be characterized by vertical temperature and salinity profiles which highlight regions of rapid change with depth as thermocline and halocline layers, respectively. Thermoclines and haloclines have been observed to form seasonally in many regions across the ocean. The specific behavior of these layers can be unique to a given location. Understanding how these layers change over time builds a foundation for studies focusing on localized primary productivity, nutrient distribution in the water column and greater Mediterranean Sea circulation patterns. Extensive temperature and salinity profiling had not yet been completed in the central Mediterranean Sea, therefore little was known about thermocline and halocline development in the regions surrounding the Maltese Archipelago. To address this, the main goal of this study was to apply CMEMS Mediterranean Sea Physics Reanalysis Product data to investigate the seasonal variability of temperature and salinity profiles in the central Mediterranean Sea at 20 locations across two transects, one between Malta and Sicily, and the other extending from Malta towards Africa. The transects cover regions with different physical features and dynamics, such that their results could be compared. The region to the north of Malta lies on a continental shelf, while the region to the south does not. Scripts were written in Matlab to plot the temperature and salinity profiles at each point from 2020 to 2022, and to identify and display the thermocline and halocline layers using the threshold method. The layers were identified using threshold values of 0.2°C/m and 0.02 PSU/m to detect the thermocline and halocline boundaries, respectively. The resulting time series heat maps showed that a seasonal thermocline formed at every point each year in early July and dissipated by December. At the same time of the year, a weak halocline formed at nearly all points, though it was stronger in the lower latitudes. The thickness of both layers changed from the time they developed to when they dissipated each year. The thermocline reached greater depths in the south than in the north. Interestingly, a permanent halocline was observed at depth of ∼150 m in both the north and south regions, but was more stable and thicker in the south where the depth was greater. This result agreed with prevailing Mediterranean Sea circulation theories. It was determined that CMEMS Mediterranean Sea Physics Reanalysis Product data can be applied to monitor variations in temperature and salinity and that seasonal changes are best visualized in the form of a time series heat map. These findings show the manner in which two physically and biologically significant parameters of sea water change seasonally throughout the water column in the central Mediterranean Sea.

Contents

List of Figures

List of Abbreviations

ADCP	Acoustic Doppler Current Profiler
AIS	Atlantic-Ionian Stream
CMEMS	Copernicus Marine Environment Monitoring Service
CMS	Copernicus Monitoring Service
CTD	Conductivity-Temperature-Depth
ERA	Environmental Risk Assessment
MLD	Mixed Layer Depth
MODIS	Moderate Resolution Imaging Spectrometer
MSC	Malta-Sicily Channel
MSPRP	Mediterranean Sea Physics Reanalysis Product
NetCDF	Network Common Data Form
OPA	Ocean Parallelize
PFL	Profiling Float
PSU	Practical Salinity Unit
SSS	Sea Surface Salinity
SST	Sea Surface Temperature

Chapter 1

Introduction

This chapter provides a summary of this research and the results that stemmed from it.

1.1 Motivation

It is no novel discovery that the ocean is changing rapidly. From marine heat waves to rising sea levels, researchers are racing to keep track of oceanic trends to best predict and adapt to the impending consequences. One method of tracking these changes is by analysing temperature and salinity profiles. Profiles show not only how important oceanic variables are changing at the surface, but throughout the entire water column. The ocean is divided into vertically stacked layers with different physical and chemical properties. Each layer may provide a unique habitat to marine life and can reflect ocean dynamics. As these layers have been known to undergo seasonal and inter-seasonal changes, it is important that they are monitored. Vertical profiling makes it possible to view these changes over time.

The seasonal patterns derived from vertical profiling have not been extensively researched in the central Mediterranean Sea. Though there are studies that address coastal thermocline development surrounding the Maltese coastline (Deidun et al., 2016), few include results representing the open ocean in the central Mediterranean Sea. Thus, it is unclear whether the thermocline only develops in coastal waters, or if it is also present in the open ocean where greater depths are reached.

1.2 Aims and Objectives

The research aims of this project are numbered from one to four and their complementary objectives are listed below the respective aim as follows:

1. Detect the thermocline and halocline layers each day at specific points to the north and south of Malta, should they exist, from January 2020 to January 2022.
   (a) Download vertical temperature and salinity data from the Copernicus Marine Environmental Monitoring Service Mediterranean Sea Physics Reanalysis Product covering a two year period from January 2020 to January 2022.
   (b) Generate a script in Matlab to plot vertical temperature and salinity profiles at specific points along transects to the north and south of Malta.
   (c) Apply the threshold method to detect the upper and lower limits of the thermocline and halocline layers for each day from January 2020 to January 2022 at each point along the transects.
   (d) Store the threshold crossing depths and plot them on the vertical temperature and salinity profiles as horizontal lines to visually represent the thermocline and halocline layers.
2. Identify any seasonal patterns of thermocline and halocline layer development between January 2020 to January 2022.
   (a) Plot two sets of time series that show the upper and lower depth limits of the thermocline and halocline layers from January 2020 to January 2022.

(b) Analyse the time series to determine the time of year when the thermocline and halocline layers became established to determine whether a seasonal pattern emerges.

3. Detect temporal changes in thermocline and halocline layer thickness at each point along the transects to the north and south of Malta.
   (a) Calculate the thickness of the the thermocline and halocline layers in Matlab.
   (b) Plot the layer thickness in time series.
4. Identify differences between the temperature and salinity characteristics of the regions to the north and to the south of Malta.
   (a) Visually compare the resulting time series from the points along the transects to the north of Malta to the ones representing the points to the south of Malta.

The present research was designed to achieve the four aims listed above. The primary aim was to detect the thermocline and halocline layers from vertical temperature and salinity data each day over two years from 2020 to 2022 along transects to the north and south of Malta. The respective objective was to produce plots of the temperature and salinity profiles at specific points along these transects which show the depth of the thermocline and halocline layers. It was hypothesized that there would be warmer water located on the surface during summer due to atmospheric heating.

The second aim of this project was to identify seasonal patterns of thermocline and halocline development. Consequently, the objective to plot two sets of time series showing the upper and lower boundaries of the thermocline and halocline layers from 2020 to 2022 was formulated. From these plots, seasonal patterns would be made visible. It was expected that the thermocline and halocline would form in the summer and disappear after fall annually.

The third aim was to detect temporal changes in the thickness of the thermocline and halocline layers. This was accomplished by completing the objective of plotting the thickness of these layers in a time series. Fluctuations in the thickness of these layers was assumed to occur in the time between their onset and disappearance.

Lastly, the current study aimed to use the results derived from the previous objectives to compare the temperature and salinity characteristics of the north and south regions. In the discussion, it will be contemplated whether the time series of each region showed different trends or different permanent features. The anticipated outcome was that the north region would have exhibited a less stable seasonal halocline and thermocline than the south, due to its bathymetry.

1.3 Proposed Solution

To address the aforementioned aims and objectives, the following solution has been proposed and implemented. This study has been conducted using E.U. Copernicus Marine Service (CMS) Information, specifically from the Mediterranean Sea Physics Reanalysis Product (MSPRP); `https://doi.org/10.25423/CMCC/MEDSEA_MULTIYEAR_PHY_006_004_E3R1`, `https://doi.org/10.25423/CMCC/MEDSEA_MULTIYEAR_PHY_006_004_E3R1I` (Escudier et al., 2020; Escudier et al., 2021; Escudier et al., 2022; Nigam et al., 2021). Temperature and salinity data covering a two year period from 2020 to 2022 was downloaded. For the purposes of the present study, averaged daily data was selected as it was sufficient for trend detection. The MSPRP data was generated by a numerical system composed of a hydrodynamic model, thus certain limitations were anticipated. These limitations are discussed in detail in the subsequent chapter. Nevertheless, the numerical model data was selected because it is open source and provides continuous coverage over a large spatial area, which was desirable for this study. It was proposed that the temperature and salinity data at each point would be plotted as a time series in Matlab to observe seasonal changes across two transects in the central Mediterranean Sea and the threshold method would be applied to detect the thermocline and halocline layers. Additionally, it was proposed that the thickness of the thermocline and halocline layers would be plotted in Matlab. In doing this, all four aims would be attainable.

1.4 Dissertation Structure

This dissertation will follow a structure commonly used to present empirical research. To begin, a background and literature overview will be provided. Information pertaining to the geography and bathymetry of the Mediterranean Sea will be included. Additionally, the general circulation of the Mediterranean Sea and the instruments used to study it will be discussed. Then the dynamics at the region of interest of this study will be specified. After narrowing down to the area of study, previous research focusing on vertical profiling methods shall be summarized. Namely, the methods applied to detect the thermocline and halocline layers are explored. Thereafter, previous studies that addressed temperature and salinity trends surrounding the Maltese islands are described. To conclude the chapter, the importance of profiling, and how it is done in practice, will be explained.

The next chapter will describe the methodology used to achieve the objectives of this dissertation. It will begin with details pertaining to data acquisition and the selection of the specific points for the analysis. Then the scripts written in Matlab that generated the vertical profiles and complimentary plots will be described in plain terms. The script written to produce the time series heat maps will be broken down as well. Next, a section justifying the thresholds selected for use in the analysis will be included. The last part of this chapter explains the script that was created to plot the layer thickness as a time series. The complete Matlab scripts can be found in the Appendix.

The presentation of the results and a discussion will succeed the methodology. This chapter starts with a summary of the types of profiles identified in different seasons. Then the observed seasonal variability will be discussed based on the results from the time series heat maps. In addition to this, the spatial variability of the temperature and salinity time series will be considered. Next, the results regarding the thickness of the thermocline and halocline layers are discussed. The chapter finishes with a discussion comparing and contrasting the results of the regions to the north and south of Malta.

The final chapter containing the conclusion will reiterate the aims and objectives of the project with a description of how each was achieved. A critique of the project, along with a short discussion of the identified limitations, will be included. Suggestions for future work and a few final remarks will signal the end of the dissertation.

Chapter 2

Background & Literature Overview

This chapter begins with a description of the physical parameters of the study region for reference in subsequent chapters. It will provide an overview of previous research and the methodologies that were applied to determine the thermocline and halocline layers. Finally, the interdisciplinary motives for monitoring these layers will be specified.

2.1 Geography of the Mediterranean Sea

The Mediterranean Sea spans a region of approximately 4,000 km by 800 km and comes in contact with three different continents: Africa, Europe and Asia; the total area occupied by this sea is 2,510,000 km^2 (Slišković et al., 2024).

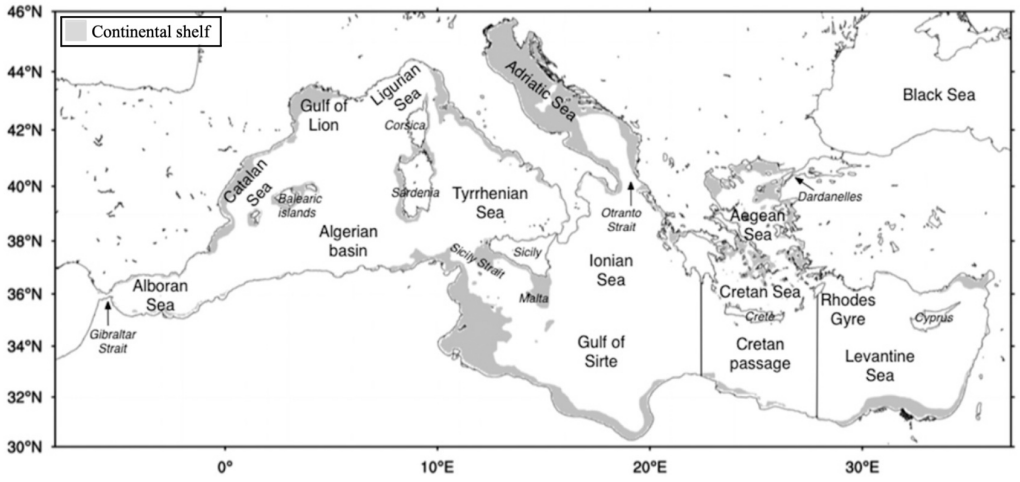

Figure 2.1: Map of the Mediterranean. Adapted from The Mediterranean Sea Overturning Circulation by Pinardi et al, 2019, Journal of Physical Oceanography, 49, p. 1700, DOI: 10.1175/JPO-D-18-0254.1. Copyright 2019 American Meteorological Society.

Figure 2.1 shows regions where the continental shelves extend from land in shaded gray. In these regions, the depth does not exceed 200 m, therefore they are considered relatively shallow considering the average depth of the Mediterranean Sea is 1,500 m (Schroeder & Chiggiato, 2023). The seafloor in the Malta-Sicily Channel (MSC) lies on top of a continental shelf, while the region south of Malta does not. This means that there is a significant depth difference between the north and south regions.

In Figure 2.2, the graduated colours show the bathymetry of the Mediterranean Sea. As can be viewed in Figure 2.2 , the Mediterranean basin is divided into two deep pools separated by the shallow Sardinian and Sicilian sills. This creates a geographical barrier between the two deep chambers. It can be observed that the east basin is larger and deeper than the west basin along this transect. In the east basin, the depth reaches a maximum of about 4,000 m, while the west basin has a maximum depth of less than 3,000 m (EMODnet Digital Bathymetry, 2022; EMODnet, n.d.). The east basin is wider than the west basin. According to this map, the ocean surrounding Malta does not reach depths greater than 450 m. Compared to the rest of the Mediterranean Sea,

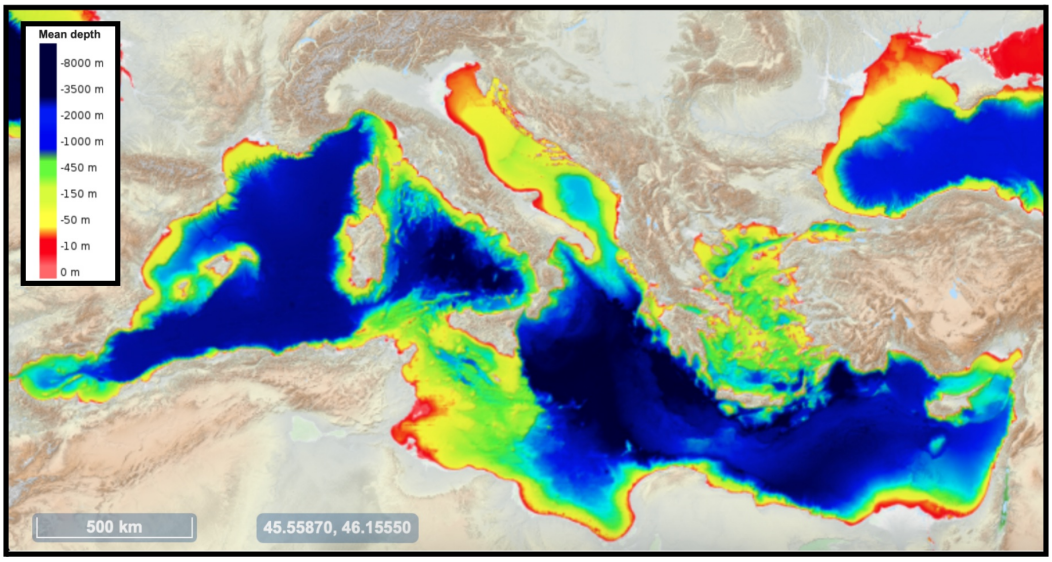

Figure 2.2: Bathymetric map of the Mediterranean Sea created using EMODnet Map Viewer using the The "EMODnet Digital Bathymetry (DTM)", which is a multilayer bathymetric product (https://emodnet.ec.europa.eu/geoviewer/).

this is a fairly shallow area. The Mediterranean Sea as a whole has a complex submarine geography, featuring trenches, sills, basins and volcanic formations (Poulos, 2020).

2.2 Circulation of the Mediterranean Sea

The Mediterranean Sea, like all other oceanic bodies of water, undergoes dynamic changes in circulation mainly driven by density gradients (Knauss & Garfield, 2016). Temperature and salinity are the two most important factors that influence density in the ocean, therefore understanding how these variables are changing can shed some light on the inner workings of greater ocean circulation patterns (Knauss & Garfield, 2016). Temperature and salinity both vary with depth, which is why they are best represented by vertical profiles (Stewert, 2008). These profiles highlight regions of rapid change with depth, which are known as the thermocline and halocline, signifying dramatic changes in temperature and salinity, respectively (Stewert, 2008). Seasonal thermoclines and haloclines are not fixed, or even develop, in all regions; the presence or lack of these features can have far reaching impacts in the ocean (Janecki et al., 2022).

Ocean currents transport volumes of water around the world's oceans. Surface and deep ocean currents are caused by different forces. Prevailing winds can create surface currents, while density gradients and bathymetry can generate currents at depth (Ocean Circulation, 2020). Currents may transport water both horizontally and vertically. They can also move in circular patterns called eddies. Numerous circular flows have been documented in the Mediterranean Sea. These can range from small eddies to large gyres. The movement of sea water is influenced by shallow sills and narrow channels, which generates complex circulation patterns. Due to its enclosed physiography, the sea water evaporation rate exceeds precipitation and runoff rates in the Mediterranean Sea, making it a concentrated basin (Romanou et al., 2010). The maximum evaporation occurs in the east in the Levantine Sea, and the minimum occurs in the west (Romanou et al., 2010). This renders the west Mediterranean less saline than the east.

As currents can undergo short term and long term changes, various instruments are required to keep track of them. Drifters are used to measure the speed and direction of surface currents by floating in a Lagrangian manner. Research by Poulain et al. (2013) implemented such a method to study surface currents in the Mediterranean Sea. Using drifter and satellite data collected between 1986 and 2012, they were able to map major currents. To the north of the Maltese islands, they recognized a current moving east through the MSC, referred to as the Atlantic-Ionian Stream (AIS) which imports relatively fresh water to the Mediterranean Sea. However, to the south of Malta, they

observed geostrophic circulation where the current moves in the opposite direction in an anticlockwise manner. Furthermore, they discovered that tidal currents exist in the Mediterranean Sea, but explained that their effects are negligible in most regions; however, they can be significant in some areas, including in the MSC.

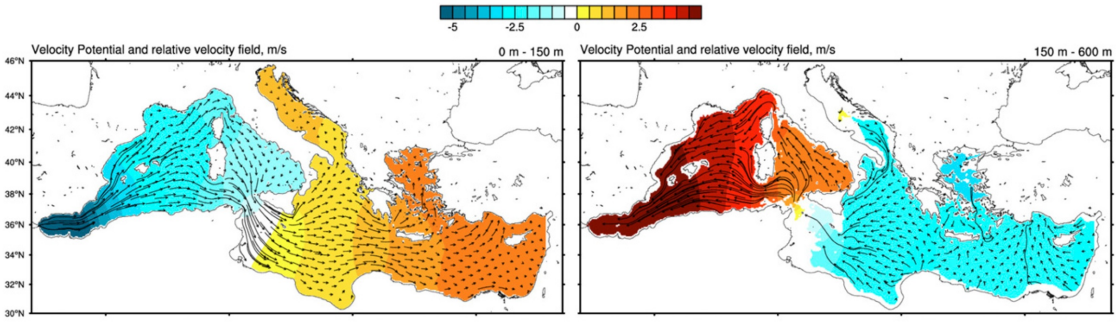

Figure 2.3: Circulation patterns in the Mediterranean Sea. Adapted from The Mediterranean Sea Overturning Circulation by Pinardi et al, 2019, Journal of Physical Oceanography, 49, p. 1715, DOI: 10.1175/JPO-D-18-0254.1. Copyright 2019 American Meteorological Society.

Figure 2.3 was created by Pinardi et al. (2019) to depict current velocities in the Mediterranean Sea. The image on the left shows the direction of flow in the upper 150 m, where the arrows represent the relative velocity field, and the colours depict the velocity potential. Similarly, the image on the left shows the same parameters for depths between 150 to 600 m.

Deep water between the east and west basins is separated by the shallow Sardinian and Sicilian sills. In general, deep water currents are weak and slow moving compared to surface currents (Ocean Circulation, 2020). This would mean that the AIS would move faster than the denser more saline water that travels out of the Mediterranean Sea via the Strait of Gibraltar. Between depths of 0 to 150 m, the velocity vector field model generated by Pinardi et al. (2019) shown in Figure 2.3 suggests that currents move eastward between Sicily and Africa. The same study revealed that currents between 150 to 600 m move westward in the same region. Additionally, their results showed that the driving forces that cause downwelling and upwelling are amplified in the MSC, where the current study is focused.

Research carried out by Zhang (2023) aimed to characterize the vertical temperature profiles associated with downwelling and upwelling. Zhang (2023) concluded that moderate upwelling is characterized by a cold-warm-cold anomaly in a vertical temperature profile. This would make sense because the cold water that settles deeper due to higher density is being driven upwards, above the warm water that is heated by the atmosphere. On the other hand, he found that moderate downwelling is identified by cold water above a warmer layer. This is logical because if downwelling occurs, one would expect the warmer surface water to be forced downward.

An example of a thermal profile that depicts a case where upwelling could be theorized to occur is shown in Figure 2.4. Figure 2.5 shows an example of a thermal profile characteristic of downwelling. If the results of this study show profiles similar to those in Figure 2.4 and Figure 2.5, it would suggest that the study region exhibits evidence of upwelling or downwelling.

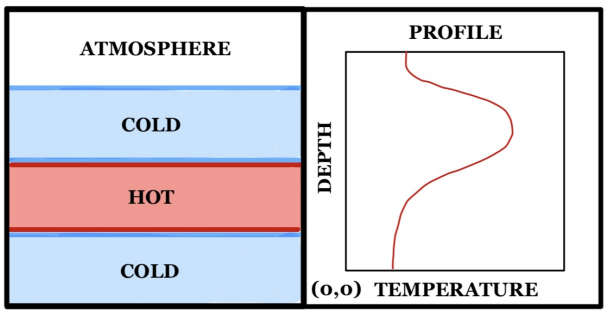

Figure 2.4: Diagram showing a thermal profile consistent with upwelling.

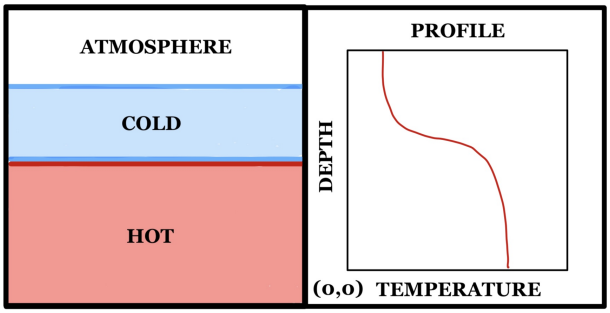

Figure 2.5: Diagram showing a thermal profile consistent with downwelling.

Deep water formation is an important part of ocean circulation. It is formed when the air temperature is cool and the surface water is very salty, causing it to sink. This process kick-starts a chain reaction that mobilizes sea water. The dense water sinks to the bottom of the ocean, and then follows the bathymetry as a river would follow a valley. In the Mediterranean Sea, deep water has been observed to form in nine areas, all of which are found in the northern part of the sea (Pinardi et al., 2023). These areas have been identified based on over 40 years of modeling and data collection. The deep water that is formed in the Levantine Sea contributes to the Mediterranean outflow water that enters the Atlantic Ocean via the Strait of Gibraltar as the AIS (Pinardi et al., 2023).

Surface currents have likely been documented more frequently in the literature because there are a wider range of affordable methods to study them. Furthermore, there are practical reasons to study these types of currents because they are referenced by seafarers, search and rescue teams and for oil spill containment. Deep water currents are not as relevant to everyday anthropogenic activities, which is why there remains limited information cataloguing prevailing currents at depth in the Mediterranean Sea.

Deep water currents are more difficult to observe from the surface. There are instruments that can collect oceanographic data at depth. Argo floats are able to move through the water column and drift with currents at depth. Additionally, Acoustic Doppler Current Profilers (ADCPs) and gliders have been used to measure deep water currents (Kassis & Korres, 2021; Mason et al., 2023). These instruments can only measure currents in localized areas, thus it is difficult to obtain continuous, widespread in-situ deep current data. The aforementioned instruments can be very costly to purchase, deploy and recover. Luckily, numeric models have improved in accuracy over the last decade, and they can be applied to study deep ocean currents.

Numeric models, though generally reliable, may not be suitable for all studies as they have limitations. For example, in regions where external forcing from hydrothermal vents influences localized circulation at depth, the model accuracy deteriorates. Moreover, since there is less in-situ data available cataloguing deep sea currents, there is less data that can be used to validate and train models. They are also limited in their ability to portray deep sea circulation by a lack of bathymetric data. As explained earlier, deep sea currents are driven by bottom topography and density gradients. Despite these issues, 3D numerical models such as those provided by Copernicus Marine Environmental Monitoring Service (CMEMS) have been shown to be accurate even at great depths. The accuracy of the MSPRP has been validated extensively by the CMS team. The results of which are published in the Quality Information Document for the particular dataset used in this study (Escudier et al., 2022). The next chapter will include a description of the ways in which numerical model data can be utilized to create vertical profiles.

2.3 Vertical Profiling Theory

The ocean is sorted into layers of sea water with varying temperatures and concentrations of salt. Fluids are sorted based on their density, and the two variables that control the density of sea water are salinity and temperature. Water with a higher salt content is more dense than freshwater, and warmer water is less dense than cold water. Therefore, cold salty water sinks while warm, less saline water floats. To better understand the layers that exist within the water column, vertical profiles are constructed. Vertical temperature, salinity and density profiles are all used to study seasonal

changes in the ocean.

In a density profile, the Mixed Layer Depth (MLD) extends from the ocean surface downward until the density rapidly changes. As its name implies, the MLD is subject to vertical mixing from wave action at the surface. Additionally, ocean circulation, turbidity, and air temperature, among other factors, can influence the depth of this layer (Treguier et al., 2023). Depending on the circumstances and location, the MLD can extend to depths ranging from a couple of meters to a few hundred (Treguier et al., 2023). This layer is biologically important because it is located in the euphotic zone where sunlight penetrates through the water column, allowing photosynthesis to occur (Janecki et al., 2022). As a result, the MLD is where most of the ocean's primary productivity occurs (Llort et al., 2019; Uchida et al., 2020, as cited in Treguier et al., 2023; Webb, 2023).

The bottom limit of the MLD marks the upper limit of the pycnocline. The pycnocline is the region of rapid density change with depth, where density is a function of temperature and salinity. To determine where the pycnocline starts, the threshold method is frequently used in the literature (Griffies et al., 2016; Janecki et al., 2022; Rivetti et al., 2017). For example, when using the threshold method in a model, Griffies et al. (2016) recommended a value of 0.03 kg/m^3 as the threshold to identify the pycnocline.

Density profiles incorporate both temperature and salinity changes with depth, where the pycnocline is the layer of rapid density change. However, it can be beneficial to study these variables separately. Vertical temperature profiles are used to identify the thermocline. As one of the most variable layers, these types of profiles are very useful to oceanographers. The thermocline is typically identified using the threshold method (Rivetti et al., 2017). Warm water is located at the surface in a layer of relatively homogeneous temperature. Below this, a thermocline may be present. If it is not, the temperature may gradually decrease with depth, or change very little (Rivetti et al., 2017). If there is a thermocline, the temperature will drop quickly, and then reach a lower temperature limit and continue to decrease gradually, signalling the beginning of the deep layer where temperatures are relatively stable throughout the year (Alvarez et al., 2021; Irmasyithah et al., 2019; Rivetti et al., 2017).

Vertical salinity profiles can show the location of the halocline layer. The top layer tends to be less saline, and salinity will increase with depth. Like temperature, salinity tends to be homogeneous in the upper mixed layer. In different parts of the ocean the halocline may be extremely weak, or non-existent. As evaporation rates increase in summer due to warmer weather, the salinity in the upper layer increases in turn.

Studying these types of profiles can provide a comprehensive view of the conditions of marine ecosystems in localized areas. Simply studying the density profile does not necessarily provide detailed information about the temperature or salinity changes with depth. It is not possible to differentiate between which variable is responsible for the density increase. It could be driven by a shift in salinity or temperature or a combination of the two. Temperature and salinity profiles better depict their individual variability with depth. For example, to monitor marine heat waves, temperature profiles are required. Alternatively, to monitor surface evaporation rates, salinity profiles may be more valuable.

In the field, Conductivity-Temperature-Depth (CTD) instruments are used to study the thermocline and halocline layers (Chubarenko et al., 2017; Hattermann, 2018; Ueno et al., 2022). These devices are very sensitive to temperature and salinity changes as they measure the conductivity of the water. To collect data, the CTD is lowered slowly down into the water column to a particular depth and then brought back to the surface. This produces vertical temperature and salinity data that researchers can convert into vertical profiles. It is not always feasible to use these devices to collect in-situ temperature and salinity data across a large area on a regular basis, but they can be used to effectively validate models (Andreu-Burillo et al., 2007).

2.4 The Thermocline Layer

The MLD has been shown to evolve with the seasons in response to atmospheric forcing (Janecki et al., 2022: Liblik & Lips, 2012). A prominent example is the onset of the thermocline. The thermocline layer's presence is dependent on various factors and its dynamics can be unique to specific regions. The thermocline has been observed in three main states. It may be permanent, semi-permanent/seasonal or non-existent depending on the location (Chubarenko et al., 2017; Irmasyithah

et al., 2019; NOAA, 2024).

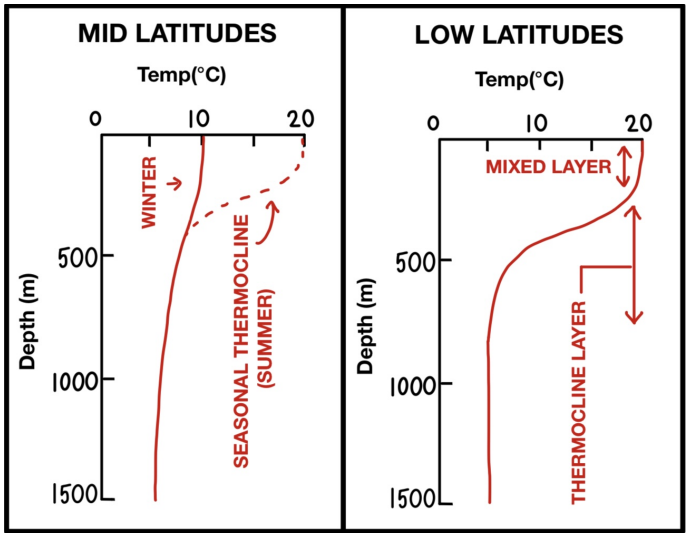

Figure 2.6: Left: diagram showing the seasonal thermocline common in mid latitudes. Right: diagram showing the permanent thermocline common in low latitudes.

In some regions, the thermocline is a permanent feature that exists throughout the entire year (Irmasyithah et al., 2019). In other regions, it can form and disappear in a seasonal cycle (Chubarenko et al., 2017), but there are also places where it does not form at all. Furthermore, it can exhibit yearly changes in addition to seasonal ones. It is believed to be a semi-permanent or permanent feature in tropical regions, and shallow or absent in the polar regions (Irmasyithah et al., 2019; NOAA, 2024). Figure 2.6 shows the seasonal thermocline often found in the mid-latitudes on the left, and the permanent thermocline typically observed in the low latitudes on the right. It can be observed from the left diagram that in the winter, the temperature throughout the water column is fairly consistent, however, in summer it is much warmer on the surface, and the temperature drops quickly with depth. The diagram on the right shows the location of the mixed layer where the temperature is uniform with depth, and it shows where the thermocline layer is.

Thermoclines have been observed to form in the open ocean in previous studies. For example, Irmasyithah et al. (2019) studied the seasonal thermocline in the Andaman Sea. They investigated the application of CMEMS Sea Surface Temperature (SST) data to study the thermocline. To accomplish this, they compared the SST data to Moderate Resolution Imaging Spectrometer (MODIS) satellite data. They found that the data from the two different sources showed similar results, with an average difference of < 1 °C. They observed that the thermocline in the Andaman Sea was shallower than 200 m during October 2017. To identify the depth of the thermocline, they assigned a threshold of temperature change with depth. The thermocline location was established based on the following temperature-depth relationship: $\Delta T / \Delta z \geq 0.1$°C/m. They generated thermal profiles at seven different stations in the Andaman Sea. Furthermore they stated that the shallower thermocline was associated with higher productivity and that seasonal changes had an effect on fish catch productivity and the location of catch (Haridhi et al., 2016; Haridhi et al., 2018, as cited in Irmasyithah et al., 2019).

In the previously mentioned study, Irmasyithah et al. (2019) identified the thermocline based on a threshold of $\geq$0.1°C/m but did not provide an explanation of how it was selected. Another group of researchers used a threshold of 0.05°C/m to mark the boundaries of the thermocline, but did not include the method used to select that value either (Tubalawony et al., 2024). Chu et al. (2023) described the gradient method as the selection of a threshold between 0.2°C/m and 0.1°C/m to determine the thermocline layer. Evidently, the literature cites many different threshold values used for determining the thermocline, though they all fall within a small range of values.

Contrarily, Janecki et al. (2022) included an extensive overview of layer identification techniques used in different types of oceans. They found that most methods for determining the thermocline and halocline depths previously tested in the literature were tested in deep water oceans, such as the Atlantic and Pacific. They were unable to find methods suitable for shallow, semi-enclosed and

brackish seas, such as the Baltic Sea where their research was planned to take place.

To solve the problem, Janecki et al. (2022) developed an algorithm that could identify the upper bound of the thermocline and halocline. Their algorithm needed to be calibrated for the Baltic Sea, thus they collected hydrographic data along a transect in the Baltic Sea using a CTD. Using this in-situ data, they were able to validate and calibrate their algorithm. EcoFish model data was used in their study and they found that the algorithm performed very well when compared to the threshold method, though they acknowledged that the success of their algorithm could have owed to the fact that it was specifically designed and calibrated for the Baltic Sea. They found that the algorithm and threshold method performed very similarly when the thermocline was well established. When the thermocline was only beginning to form, the threshold method was not as accurate. It was observed that both methods accurately identified the halocline consistently, as this layer tends to be fixed throughout the year in their study region. They produced a time series from the model data showing the average daily thermocline and halocline depths over a seven year period. The time series showed a pattern of seasonal changes in the thermocline. It started to develop in May, and deteriorated after December. The halocline remained at a stable depth throughout the year, thus no seasonal variability was observed in their study region. They concluded by stating that they believed the algorithm could be applied to other seas, provided that the proper steps were completed to calibrate it for the desired region. This article demonstrated that there are other methods that can be used to find thermocline and halocline depths besides the common threshold method. It is up to the researchers to determine which method is best suited for their study region considering the resources available to them.

To highlight the potential shortcomings of the threshold method, Treguier et al. (2023) showed how slight differences in density threshold values can impact the identified depth of the mixed layer. They used a diagram to show how the general shape of the MLD differs seasonally, and how a chosen threshold may lead to the misidentification of the boundary layer. By setting slightly different thresholds of 0.01 kg/m^3 and 0.03 kg/m^3 they found a difference of 200 m in the MLD during spring.

They also discuss the purpose of using a reference depth when seeking to determine the depth of the MLD or the thermocline. Typically, when analysing observational data, researchers will set the reference depth to 10 m to avoid misidentifying a certain layer due to short term fluctuations. However, depending on the threshold, the reference depth may need to be adjusted. It can be assumed that if the threshold used to identify the MLD can impact the results so significantly, the same must be true in selecting a threshold to identify the thermocline.

2.5 The Halocline Layer

The halocline is the layer where ocean salinity changes rapidly with depth (Janecki et al., 2022). Above the halocline, there tends to be a homogeneous distribution of dissolved salts due to mixing. The stability of the halocline is dependent on the climate of the region. Factors that can alter the salinity include amount of rainfall, evaporation and run-off. Certain regions experience higher volumes of precipitation during certain seasons, which could cause the halocline to temporarily shift position.

A particular study by Ueno et al. (2022) investigated the inter-annual variation in the winter halocline on a global scale. To do this, they analysed salinity profiles from the World Ocean Database 2013 in conjunction with Profiling Float (PFL) and CTD data. They collected almost 200,000 profiles from 2000 to 2017 from these different databases and normalized them into profiles with 10 m intervals. From this data, they were able to map the halocline strength and depth across the world's oceans with a grid resolution of 4°x4°. They found that a well established halocline could be found when Sea Surface Salinity (SSS) was low. Their findings showed that the halocline was absent in central subtropical oceans, but was consistently observed between 20°S and 20°N latitudes. The study region of this dissertation does not fall within these limits. Between 20°S and 20°N latitudes, they found that the halocline was normally located at depths shallower than 100 m. Their study categorized haloclines in certain regions according to their strength. They defined halocline strength with thresholds in units of Practical Salinity Units (PSU) per meter, where a strong halocline would be given by a value of > 0.05 PSU/m, a moderately strong one by > 0.03 PSU/m, and a weak one by 0.01-0.02 PSU/m . For each normalized profile, they calculated the salinity gradient as the

change in salinity per unit depth ($\Delta S/\Delta D$) to identify the halocline. They then took the average halocline depth for each 4°x4°box. When the halocline strength and depth were great, so was the standard deviation within the averaged box.

In their paper, Ueno et al. (2022) state, "The halocline is expected to be strong in areas where the salinity above the halocline is low and/or the salinity below the halocline is high". This is logical because it would imply that there must be a significant difference in the salinity between the layer above and below the halocline. They noted that the halocline strength demonstrated annual and spatial variability. Their data showed that the average halocline depth in the central Mediterranean Sea was between 75 to 100 m and the halocline strength was weak to moderately strong.

2.6 Importance of Vertical Profiling

Identifying and understanding the seasonal patterns that occur in the ocean will help researchers better predict migration patterns, phytoplankton blooms, and other marine phenomena (Aspillaga et al, 2017; Chu & Fan, 2020). If the water column exhibits a predictable seasonal pattern of thermocline and halocline depth it will be easier for researchers and policy makers to predict when species are most vulnerable in the areas surrounding Malta, and could aid in the implementation of regulations to protect marine life as they pass through sensitive areas. It is well known that the MSC is one of the most heavily trafficked shipping routes in the Mediterranean Sea, thus it is exposed to a number of additional pollutants and hazards that could threaten marine life (Di Lorenzo et al., 2017). Imposing seasonal laws may be a viable solution.

Temperature and salinity profiling provides researchers with important insights into global and regional ocean circulation. Profiling can be done in various ways, but one purpose of profiling is to identify regions of rapid change in physical variables. Owing to their physical and biological implications, temperature and salinity are variables of particular interest (Alvarez et al., 2021). These variables also control the density of sea water. Differences in density create gradients which drive oceanic circulation. This explains why previous research has focused on monitoring temperature and salinity with depth. In doing so, one can easily identify the thermocline and halocline. These features are dynamic and shift vertically through the water column in response to driving forces, such as air temperature, salinity and currents.

The formation of thermocline layers can affect nutrient distribution in the water column; Jean-Baptiste et al. (2017) studied the effects of seasonal variability of the thermocline on nutrient distribution. They found that essential nutrient levels change with temperature in a polynomial fashion. They collected vertical nutrient and temperature data along the coast of Africa in 2009 for their analysis. From this, they determined the thermocline, oxycline, phosphacline and nitracline minimum and maximum depths for a 12 month period. This allowed them to view the differences in depths between seasons. They found that the thermocline acts as a barrier that prevents the ascent of nutrients, thus limiting productivity. When the thermocline is shallow, so are the nitracline and phosphacline. This tends to be the case in the winter when the vertical mixing is high. They discovered that the distribution of dissolved oxygen cannot be measured as a function solely of temperature, but must be studied as a combination of factors including biological activity and atmospheric forcing. They concluded by stating that the nitracline and phosphacline depend on the depth of the thermocline. Similarly, Alvarez et al. (2021) studied the seasonal thermocline's effect on the vertical distribution of fish larvae; they found that the larvae of certain fish species are more highly distributed below the thermocline, while others are more commonly found above it.

Thermocline depth is studied by meteorologists to better predict the severity of hurricanes (NOAA's National Ocean Service, n.d.). These destructive storms are generated over the ocean as warm surface water evaporates and condenses into clouds that pick up speed and energy as they travel landward. The thermocline depth determines how much warm surface water is stored in the hurricane's reservoir (NOAA, 2024); the larger the reservoir, the greater the hurricane. As ocean temperatures increase the thermocline layer may become deeper causing more extreme hurricanes.

These many examples have demonstrated how the study of the thermocline can benefit multiple additional studies in the field of oceanography. The thermocline has climatological, biological and physical research applications, thus the development of an open-access script to visualize its seasonal variability can benefit a wide range of stakeholders. Additionally, it was made plain that though many studies have been conducted on the topic of the thermocline and halocline, there are few that

address the central Mediterranean Sea and the seasonal patterns that occur there.

2.7 Thermocline and Halocline Detection Theory

Relatively little is known about the thermocline and halocline seasonal cycles that occur in the central Mediterranean Sea because extensive vertical temperature and salinity profiling has not been conducted in this region. This could be because in-situ data collection can be costly and time consuming. Continuous vertical temperature data is collected by submerging temperature loggers attached to moorings. This can be feasible in shallow areas, but in the open ocean it is not practical for multiple reasons. Firstly, the mooring may drift or drag along the bottom due to strong currents or storm surges. This would change the position of the loggers. Secondly, even if the mooring did not drag, it is possible that currents could prevent the line from maintaining perpendicular positioning to the sea floor. As a consequence, unknown and potentially significant depth errors would be introduced. A third issue is the cost of temperature loggers; as ocean depth increases, so does the number of loggers needed to detect temperature variations. Depending on funding, researchers may not be able to justify spending large amounts on loggers. Finally, the temperature loggers must be retrieved to access the stored data. This would not be possible if the mooring had detached or been removed. Therefore, to collect in-situ vertical data, researchers must have access to sufficient funding and resources to install and retrieve the loggers at sea.

As described earlier, CTDs can also be used to collect vertical profile data (Chubarenko et al., 2017; Hattermann, 2018; Ueno et al., 2022). However, there are limitations to this method as well. These devices are quite expensive, and to obtain continuous data to analyse seasonal variability, data must be collected frequently. As a study like the current one is conducted in the open ocean, this would require access to a vessel and crew to transport the CTD to the locations of interest. This would be both time consuming and expensive.

With new leaps in algorithm development over the past few years, there are many reliable numerical ocean models available, which researchers can use as an alternative to costly in-situ data collection (Kamenkovich, 2004). Namely, the CMEMS MSPRP has been applied in this study to collect vertical temperature and salinity data at sites to the north and south of the Maltese Islands.

In a coastal study of Maltese waters conducted by Deidun et al. (2016), temperature data was collected through the installation of six temperature loggers along a mooring line. They investigated the effectiveness of using Ocean Parallelize (OPA) model data versus satellite data to approximate sea temperature, while using the in-situ temperature logger values for reference. This was a comparative study to determine whether model or satellite data is best suited for predicting sea temperatures in coastal areas. They found that both the satellite and model data can be applied to predict water column temperatures up to a depth of 42 m during winter and spring. They determined that when the thermocline is present in the summer and fall, the model and satellite data deviate from the in-situ temperature values. However, they concluded by stating that model and satellite data can both be used to identify seasonal variability in the thermocline and its relative thickness. Additionally, they discussed the seasonal variability in the thermocline that they observed in coastal Maltese waters. This is relevant to the current study because it investigates the seasonal thermocline to the north and south of Malta. Their findings have demonstrated that model data has applications for identifying seasonal changes in the thermocline, though it does not investigate it in the open ocean. The results of the present study will later be compared to the thermocline trends that they observed in the coastal regions surrounding Malta. Their results showed that the thermocline was not established in the winter and spring, but exists during the summer and fall seasons in coastal waters.

As technology advances and numerical models become more reliable and accessible, vertical profiling can be accomplished in remote locations. This study has been conducted using data from CMEMS. This service offers a wide range of data, including vertical temperature and salinity data. All products are open access and available for download at www.marine.copernicus.eu. The specific model that was used as a source for data in this study is the CMEMS MSPRP (Escudier et al., 2020; Escudier et al., 2021; Escudier et al., 2022; Nigam et al., 2021). This product contains 3D hourly, daily, monthly and yearly temperature and salinity data covering the entire Mediterranean Sea. It consists of 141 unevenly spaced depth levels stretching from the ocean surface to 5754 m, and a spatial resolution of 0.042°x 0.042°(Escudier et al., 2020; Escudier et al., 2021; Escudier et

al., 2022; Nigam et al., 2021). The specific depth value of each level of this model can be found in Appendix B. The model was calibrated based on in-situ temperature and salinity profiles, sea surface temperature and sea level data. The dataset is updated monthly to account for the spin-up time and to incorporate new in-situ measurements. This product has been documented in use cases to conduct Environmental Risk Assessments (ERAs) of oil spills and to analyse extreme wave heights (ARTELIA Group, n.d.; Bonvicini, n.d.). It has been proven as a reliable source that is constantly being updated.

Using the CMEMS MSPRP dataset, this thesis investigates the seasonal variability of salinity and temperature profiles in regions north and south of the Maltese islands. In the subsequent methodology section of this report, a description of the steps taken to generate the scripts used to identify the thermocline and halocline in Matlab can be found.

Chapter 3

Methodology

In this chapter, the methods applied to complete this study will be explained. First, the data acquisition process will be described, including the reasoning behind selecting the specific data point locations. This will be followed by an overview of the core script functions designed in Matlab. Specifically, the three most important scripts which each orchestrated a unique and essential operation will be broken down; these include the vertical profiling script, the heat map time series script and the layer thickness script. Following this, the use of these scripts to select the values of the thermocline and halocline thresholds will be explained by showing examples of produced plots.

3.1 Data Acquisition

Vertical temperature and salinity data was downloaded as a Network Common Data Form (NetCDF) file from the CMS. More specifically, two years of sea water potential temperature and sea water salinity data was downloaded from the MSPRP. Two separate files for the north and south were acquired using the download by polygon tool on the Copernicus browser. Rectangular polygons were drawn to cover the entire regions of interest: the region between Malta and Sicily and the region between Malta and Africa. The exact coordinates that would describe the polygons are not important. This owes to the fact that only specific points would be used in the analysis. As long as the polygons encapsulated these points, it did not matter what the size or shape of them was. It would have been sufficient to download data for specific points directly, however, at this point in the project the exact points had not been selected. The selection of these points will be explained in the following section.

3.2 Transect and Point Selection

Once the file properties were made visible in Matlab, the longitude and latitude data was read. A transect between the southern coast of Sicily and Malta, in line with the capital city of Valletta, was chosen. The closest longitudinal increment to Valletta was located at 14.5417°E. Along this transect, 10 points were selected to observe the differences in salinity and temperature based on proximity to the coast and depth. The points to the north of Malta lie on the continental shelf, where depths do not exceed 200 m. As the spatial resolution of this dataset is given by 0.042°x 0.042°, a latitudinal increment of 0.084° was chosen to evenly distribute the points between Malta and Sicily. This would allow one to observe whether a thermocline and halocline forms regardless of proximity to the coastlines, as had been observed in a previous study (Deidun et al., 2016). Similarly, 10 points were chosen to the south of Malta in line with the northern transect with the same spacing as those in the north for consistency. In the south, depths exceed 600 m, therefore it shows whether these layers form regardless of depth in the central Mediterranean Sea. The selected points can be visualized in Figure 3.1b. As can be viewed by Figure 3.1, the study region is located in the central Mediterranean Sea, between Sicily and Africa. The latitudes range from 36.7292°N to 35.0208°N, covering a distance of ∼190 km.

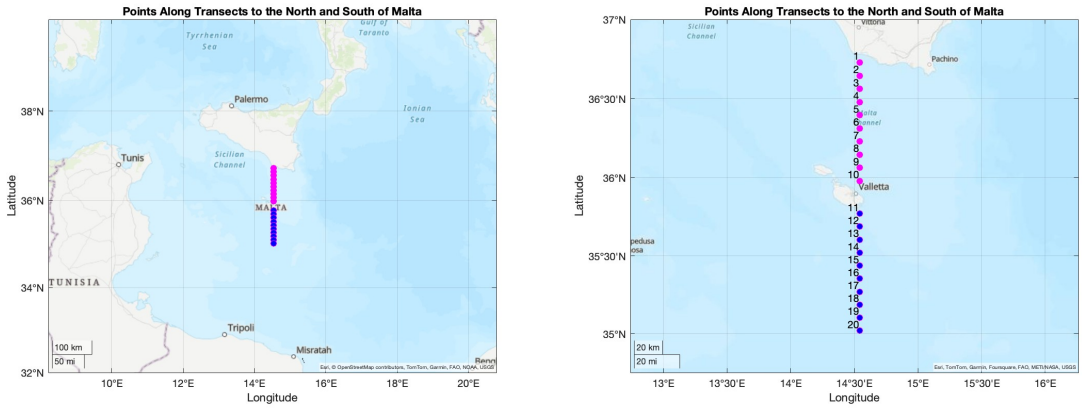

(a) Study region

(b) Transects

Figure 3.1: Points along the transects.

3.3 Vertical Profiling

The script to compute and plot the thermocline and halocline layers was written in Matlab. This simply plotted the temperature or salinity against depth for a given data point. To test the script was working properly, a single point along a transect was selected. The depth and temperature data at point 7 was read in Matlab. The vertical temperature was plotted against depth on September 10th, 2020 at this point. However, since the thermocline must be calculated based on a threshold of the temperature gradient with depth, the temperature profile had to be converted to a gradient profile. The change in temperature per unit depth was calculated between each interval and plotted. This was done by incorporating an element to the script that would take the difference in either temperature or salinity between data points and divide it by the difference in depth. The resulting plots are shown in Figure 3.2.

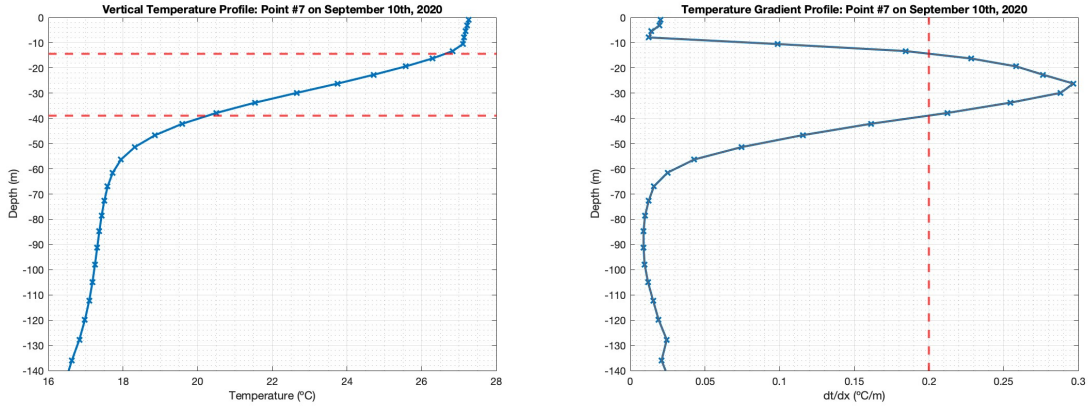

(a) Temperature profile

(b) Temperature gradient profile

Figure 3.2: Profiles at point 7 on September 10th, 2020.

The blue X's in Figure 3.2a and Figure 3.2b show the vertical depth intervals of the dataset. As the MSPRP does not provide continuous data, the gaps between points needed to be approximated. A linear interpolation was completed in Matlab to create a continuous dataset. This was done by calculating the equation of a line between each point and finding the corresponding gradient for every depth along that line in Matlab. This provided corresponding temperature data for each depth. After this step had been completed, all that remained to find and plot the thermocline was to select a threshold of the gradient. In Figure 3.2b, a threshold value of 0.2°C/m is identified using

a vertical red line. When this threshold was crossed by the blue gradient curve, the script then calculated the exact depth where it was crossed and plotted this value on the temperature profile shown in Figure 3.2a. In this example, the gradient threshold was crossed at two depths. This is represented by the upper and lower limits of the thermocline plotted as horizontal red lines in Figure 3.2a.

Ideally, one would expect the script to identify either two or zero threshold crossings. In the case of two crossings, the thermocline would be present with an upper and lower boundary, and if there were no crossings, the thermocline would not exist. However, the results showed that for a given threshold, there could be between zero and six crossings detected within the dataset. Figure 3.3 shows an example of such an instance when more than two crossings was observed.

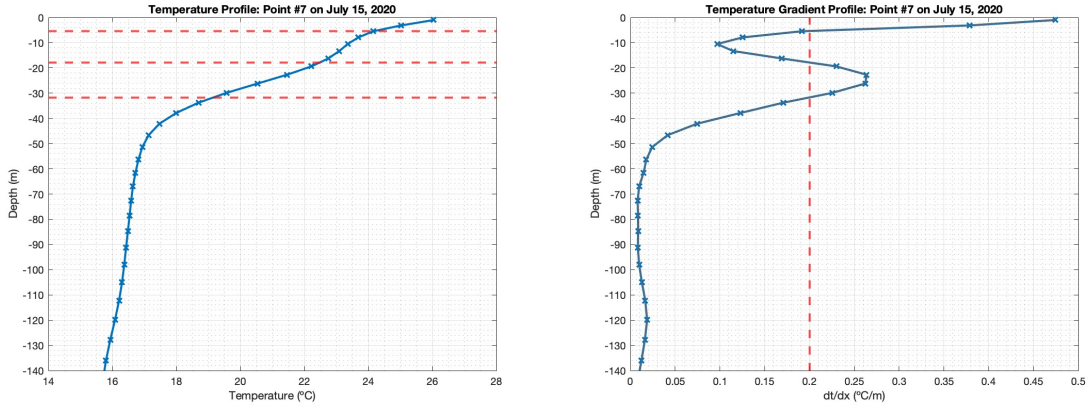

(a) Temperature profile

(b) Temperature gradient profile

Figure 3.3: Profiles at point 7 on July 15th, 2020.

In Figure 3.3b, there are three depths where the gradient threshold is crossed. This meant that the method of identifying and plotting the thermocline layer had to be adjusted. The script was modified to store and plot the number of threshold crossings.

3.4 Generating the Time Series Heat Map

After generating a vertical temperature profile for a single point on a single day, a script was written to generate profiles for all points on all days. This was done by creating a loop to repeat the calculations and plots. The challenge was to find a way to represent this data as a time series. From the previous profile script, a plot was generated for all dates for point 7 in the north. The result is shown below in Figure 3.4.

Clearly, this plot was far too cluttered to be able to interpret, so a different approach was required. A new script was written in Matlab to produce a time series heat map. The script first read the depth data, which did not change between days, and converted the temporal data from a numerical format to a string using specified start and end dates. For the dataset, the start and end dates were 01/01/2020 and 01/01/2022, respectively. The temporal data was displayed along the x-axis, consistent with a time series format. As 10 points were to be analysed in the north, a tiled layout function was applied to generate plots for each point within a loop. A second loop was incorporated to display the data for the entire two year period by adding one day at a time to the time series. A mesh grid was created to display a heat map showing the variation in temperature with depth over time. The mesh grid was interpolated to smooth the coloured heat map and provide a better visualization of continuous temperature variation. A colour bar type “Jet” was selected to intuitively represent the temperature range from cold to hot with blue signalling colder temperatures and red signalling hotter temperatures. The depths where the threshold was crossed on each day was plotted on top of the time series heat map using the scatter function. On the days when there were two threshold crossings, these depths were overlaid on the heat map as markers. An example of the resulting plot is shown in Figure 3.5 for a threshold value of 0.2°C/m at point 7. The blue markers show the upper boundary of the thermocline layer, which is also known as the first threshold

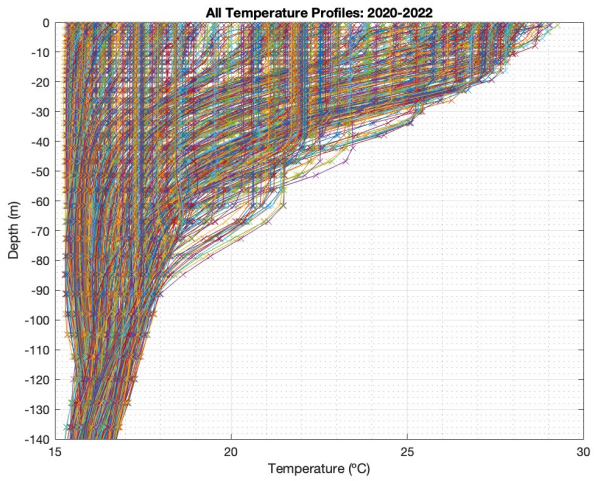

Figure 3.4: All vertical temperature profiles.

crossing. The red markers show the lower limit of the thermocline. The same approach was used to plot the halocline using the vertical salinity data.

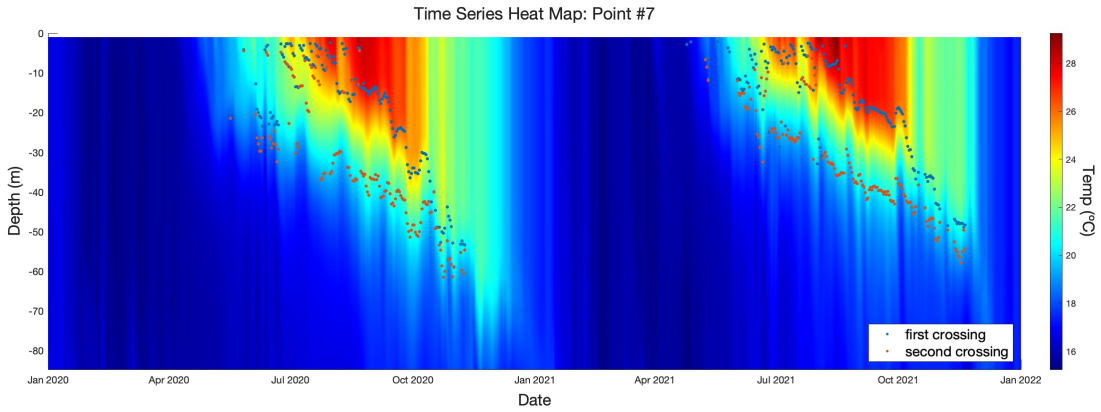

Figure 3.5: Time series heat map at point 7.

3.5 Determining Optimal Threshold Values

As there was little information regarding the threshold selection processes in the literature, a brief investigation was performed to select the optimal value. Various sources referenced the use of slightly different threshold values. Therefore, thresholds ranging from 0.1 to 0.4°C/m with an increment of 0.05°C/m were tested with the CMEMS MSPRP data. The script searched for instances where the threshold value was crossed. If it was crossed, this would signal a boundary of the thermocline. A well established thermocline should have an upper and a lower limit, thus one would expect there to be two crossings for a given profile, or zero if the thermocline is not present. Ideally, there would be either two or zero crossings, but in reality the dataset showed between zero and six crossings over the two year period across the selected points. In selecting the optimal threshold, the number of crossings that are not equal to zero or two should be minimized. An example of the resulting time series are shown in Figure 3.6.

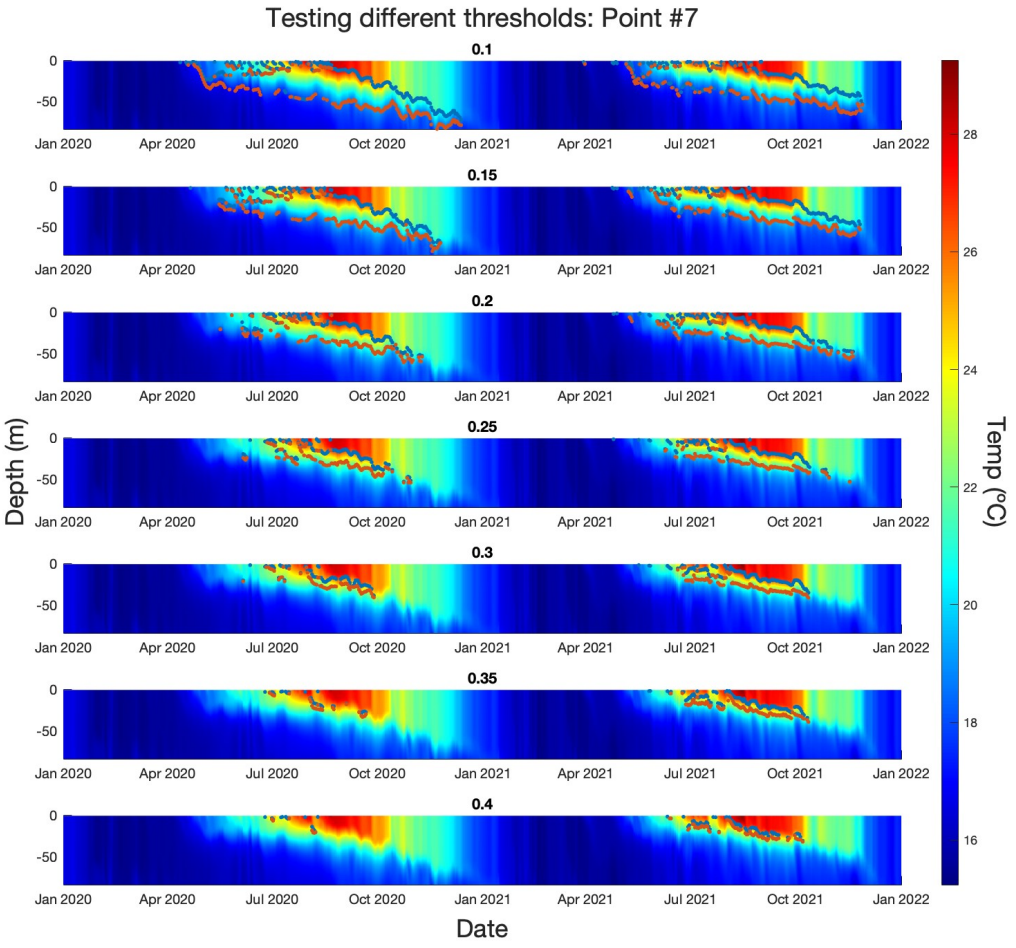

Figure 3.6: Testing threshold values at point 7.

An additional script was written to count all crossings for different threshold values and display the results as in a bar chart. An example of the resulting chart is shown in Figure 3.7.

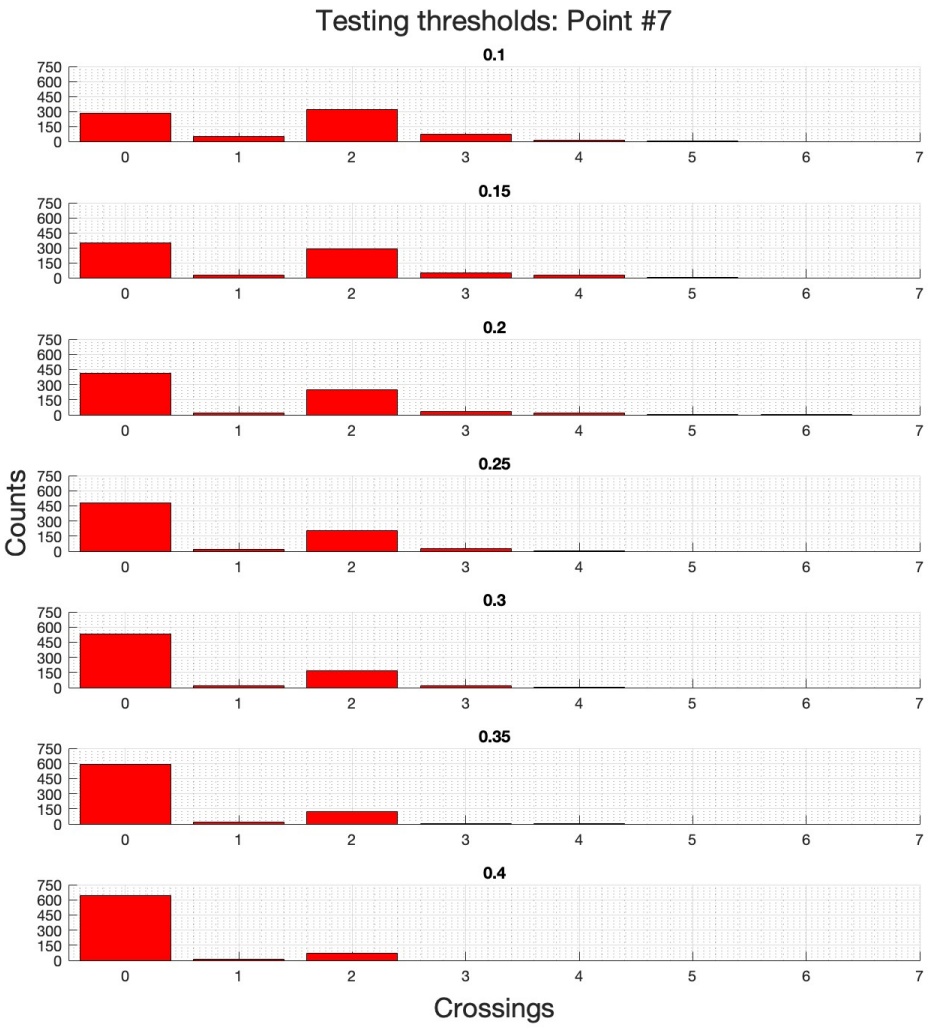

Figure 3.7: Bar graph showing counts for each number of crossings at different thresholds at point 7.

The detailed results of this investigation will be discussed in the first section of Chapter 4. In any case, based on the information provided by the bar chart and time series, a threshold value of 0.2°C/m was selected to be applied for thermocline detection. This was the final step to finish the script which produced the plots to be analysed. The same methodology was used to select the threshold to detect the halocline by testing values between 0.01 PSU/m and 0.05 PSU/m with an increment of 0.01 PSU/m. From the information provided by these graphs and the literature, a threshold value of 0.02 PSU/m was selected to identify the halocline.

3.6 Plotting Layer Thickness

Another aim of this thesis was to plot the thickness of the thermocline and halocline to observe whether seasonal changes occur. A separate script was written to calculate the thickness of these layers by taking the difference in depth between the first and second crossings. This only plotted the thickness for days where there were exactly two crossings, with the first being the upper boundary, and the second being the lower boundary. An example of the resulting plot is shown in Figure 3.8.

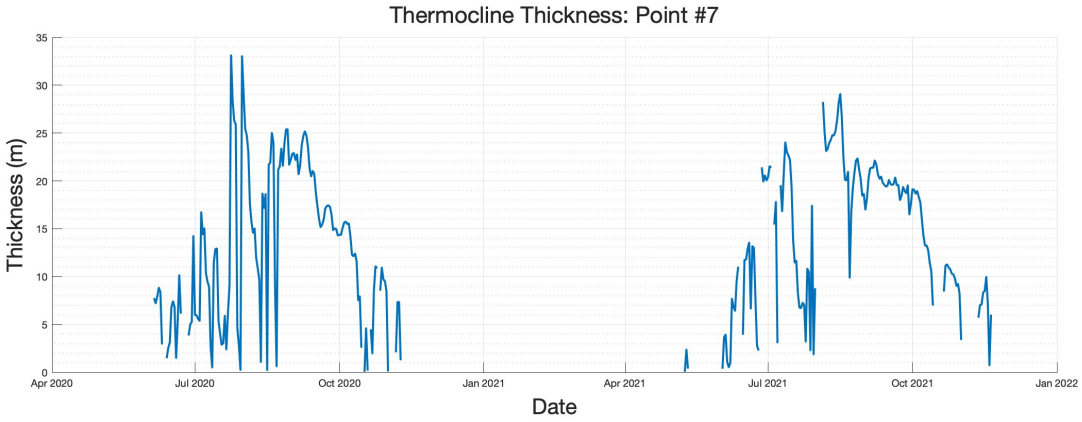

Figure 3.8: Thickness of the thermocline plotted over two years at point 7.

The complete scripts used to generate these plots can be found in the Appendix. The results of these plots will be discussed in following chapter.

Chapter 4

Results & Discussion

In this section, the results of this study will be analysed in detail. The motive of this study was to determine whether the thermocline and halocline undergo seasonal changes in the central Mediterranean Sea. Furthermore, it aimed to establish if there were any observed temperature or salinity differences between the regions in the north and south. To address these questions, first the results pertaining to the thermocline and halocline layers will be explored. Then any differences between the north and south regions will be examined.

4.1 Temperature and Gradient Profiles

A simple vertical temperature profile was produced in Matlab for a given day and position. An example of which was shown in Figure 3.2 in the methodology section. The same image is shown below in Figure 4.1. The threshold that was selected to detect the thermocline layer was 0.2°C/m based on the plots that compared commonly used values in the literature. A visual analysis of Figure 3.6 and other examples for different points was conducted. It was assumed that the best threshold would position the upper boundary of the thermocline, the blue dot markers, just below the red portion of the heat map, and the lower boundary, the red dot markers, where the dark blue layer reappeared. This would encompass the depths with the greatest range in temperature. Additionally, bar charts were produced to show the distribution of the number of crossings for different thresholds. An example was shown in Figure 3.7. If the thermocline was well established, there would be two crossings, and when it did not form, there would be zero crossings. If the counts for two crossings exceeded the number of counts for zero crossings, it would mean that a thermocline was present during the majority of the year. Figure 3.7 also highlights the point made by Treguier et al. (2023) in their paper which discussed the shortcomings of the threshold method. As can be observed in Figure 3.7, very slight alterations of the threshold can produce very different results. In an attempt to further narrow the threshold value to more accurately detect these layers, another article was referenced; a previous study conducted near the Maltese coastline showed that the thermocline was only present in the summer and fall months (Deidun et al., 2016). This information was used to study the point nearest the Maltese coast, point 10, where it could be assumed that the thermocline would exist in the summer and fall months only. The threshold value that produced a ratio of approximately 1/3 of the total counts for two crossings and 2/3 the total counts for zero crossings was selected. This would mean that the thermocline would exist for approximately four months of the year. From these results, the threshold that appeared to best identify the thermocline layer was 0.2°C/m.

The script produced a vertical temperature profile at point 7 on September 10th, 2020. This date and location was selected to view the profile trend when the thermocline was hypothesized to exist. The resulting plot showed that near the surface, the temperature of the water was ∼27°C. As the depth increased to 15 m, the temperature did not change very much, but after this, the temperature declined almost linearly until it reached a value of ∼20°C at 40 m, thereafter it gradually declined until the maximum depth was reached. The threshold is shown on Figure 4.1b by the vertical red line. It can be remarked that the threshold was crossed by the gradient curve twice. First, the threshold was crossed at a depth of ∼15 m and then again at ∼40 m. These depths are shown on Figure 4.1a as horizontal red lines. The area between them represents the thermocline layer.

The gradient plot in Figure 4.1b showed that the temperature change with depth was greatest within the thermocline layer. This is what one would expect based on the previous profile. It revealed that the temperature change increased from the surface until it reached a maximum rate of

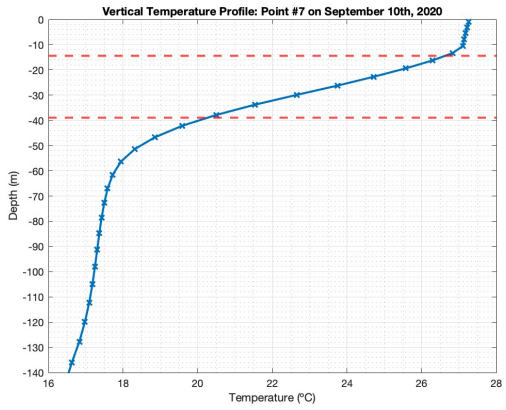

(a) Temperature profile

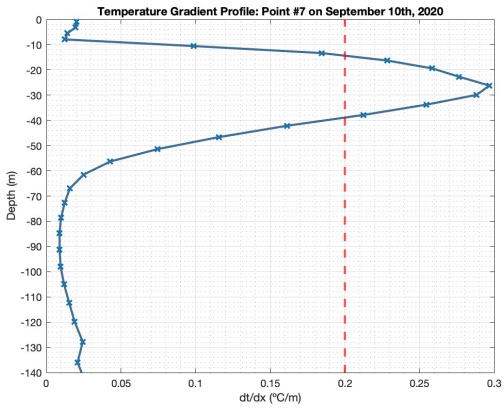

(b) Temperature gradient profile

Figure 4.1: Profiles at point 7 on September 10th, 2020.

change of 0.3°C/m at ∼30 m, then it decreased to approximately zero change near the 70 m mark. Again, this is in line with the previous profile. It indicated that the script was working properly.

Following this, several other dates were tested to view the different types of vertical temperature profiles and respective gradient profiles that occurred throughout the year with the same threshold.

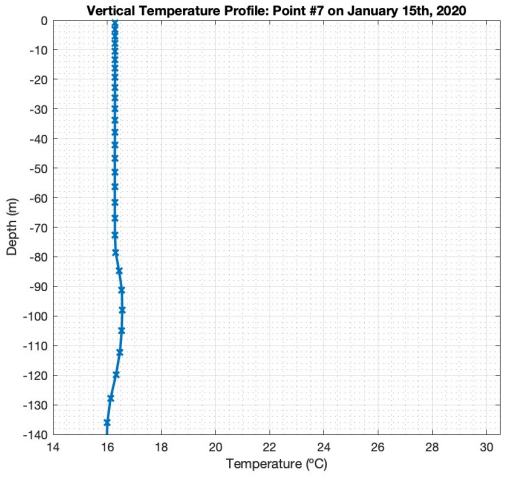

(a) Temperature profile

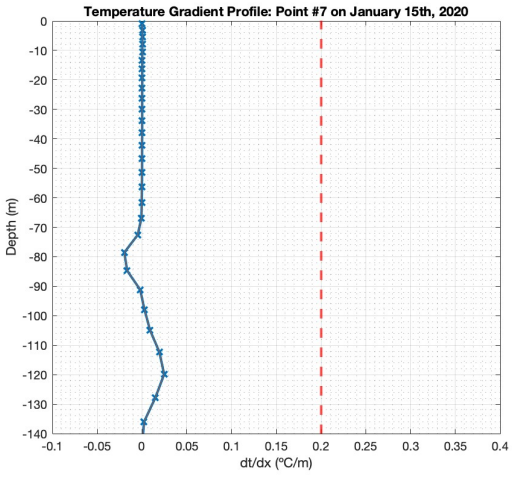

(b) Temperature gradient profile

Figure 4.2: Profiles at point 7 on January 15th, 2020.

A winter date was selected to view the profile when the thermocline was not expected to exist. Figure 4.2 shows that this was indeed the case. In Figure 4.2a which shows the temperature profile on January 15th, 2020 at point 7, there was hardly any notable temperature change between depth intervals. This profile indicates that there was no thermocline present at this time. Furthermore, in viewing Figure 4.2b of the corresponding gradient profile, it is clear that the threshold was not approached at any depth. There were a few slight disturbance in the gradient after 70 m, but otherwise it remained fixed with a value of zero, meaning there was no change in temperature with depth.

Through this method of testing different dates, it became apparent that there were dates when the thermocline was not present, such as on January 15th, 2020. On such dates, the vertical profiles did not show a curve characteristic of a thermocline, that being a rapid temperature decrease with depth, followed by reaching an asymptotic minimum temperature barrier. Near the time when the thermocline was expected to develop, a distinctly different profile was observed. In this profile type, the temperature gradient oscillated around the threshold value, causing the detection of more than

two threshold crossings on a given date. An example of such a profile was shown in Figure 3.3. One possible explanation of this result could be vertical mixing of the water column triggered by weather events. Another could be horizontal currents transporting colder or warmer water through a given point.

4.2 Seasonal Variability of the Thermocline

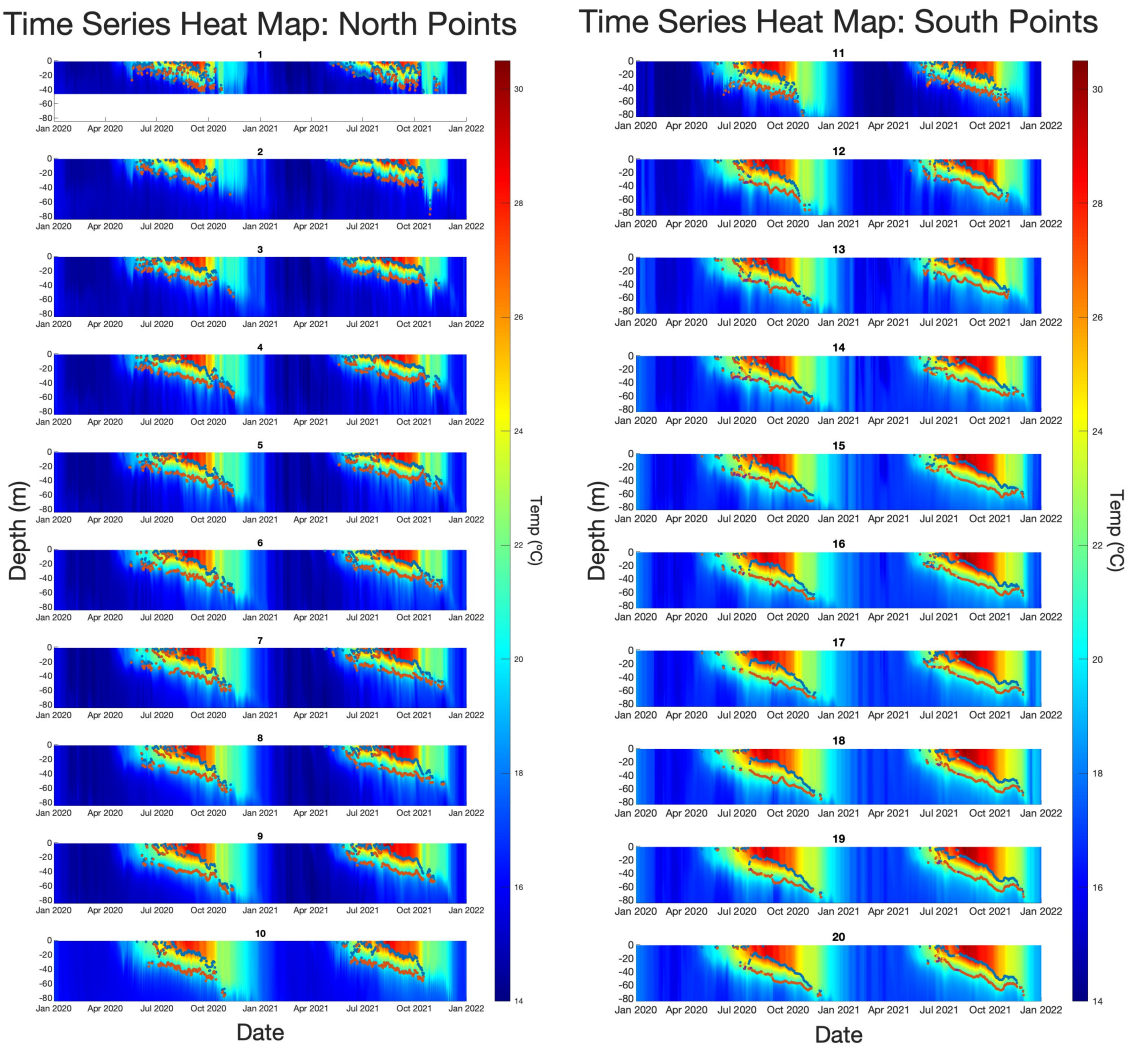

(a) Time series heat map: north points

(b) Time series heat map: south points

Figure 4.3: Time series heat maps showing temperature variation with depth from 2020 to 2022.

Time series heat maps were produced for each of the 20 points, making it possible to observe whether any seasonal variability occurred. It was hypothesized that the thermocline would only exist in the summer and fall months. As explained in the previous chapter, the vertical temperatures for a period of two years starting from January 1st, 2020 were plotted. Each time series is shown in Figure 4.3. In studying these results, there was a clear pattern of thermocline development. In January, the temperatures throughout the water column did not vary with depth. This did not change until around June, when the water temperatures near the surface began to warm. This marked the onset of the thermocline layer. The surface water temperatures continued to warm, and the warmer water was observed to reach greater depths as the summer progressed. By July,

the time series started to show the warmest temperatures near the surface, and a rapid decline in temperature with depth. After October, there was an abrupt absence of thermal stratification, though the sea temperature remained relatively warmer until around December, at which point it returned to an isotropic minimum temperature. This could have been a result of increased mixing of the water column in the fall months, leading to a uniform temperature throughout the water column. The thermal energy could have been redistributed by the mixing, which would explain why the warmer temperature reached even greater depths, and the warmest surface water observed before October suddenly dissipated. These results agreed with the hypothesis that the thermocline would be observed solely in the summer and fall.

The aforementioned results agreed with the findings of Deidun et al. (2016) that were presented in their coastal study of the thermocline surrounding the Maltese islands. They found that the thermocline existed only in the summer and fall. The same was discovered to be true not only near the coast, but also in the open ocean to the south of Malta and across the entire MSC. During this period, the thermocline layer shifted to greater depths later in the season.

As discussed in the literature review, Irmasyithah et al. (2019) observed that the thermocline layer was shallower than 200 m during the transitional month of October in their study region which was located in the Andaman Sea. The transitional month observed at the current study region appears to be November, and the thermocline does not reach depths greater than 80 m at any of the points. Irmasyithah et al. (2019) stated that a shallower thermocline promotes productivity, therefore the most productive times in this region would theoretically be during the early onset of this layer in June; however, productivity is also limited by nutrient availability, dissolved oxygen and solar radiation, thus this may not be the case.

4.3 Temperature Variation Between Points

In the previous sections, the individual and collective temperature profiles were discussed. It was observed that the thermocline layer varied seasonally across all points. In this section, the spatial variability of the thermocline layer will be analysed. Figure 4.3a and Figure 4.3b show the temperature and thermocline differences between each point in the north and south, respectively. Only the upper 84 m are shown in these Figure 4.3a and Figure 4.3b because there were no visible temperature changes in the water column beyond that depth. This allowed the thermocline layer to be viewed in more detail. Each time series is numbered in accordance with Figure 3.1b. In Figure 4.3, the blue markers depict the upper limit of the thermocline on a given date, and the red markers correspond to the lower limit. In the north, point 1 showed that the thermocline extended to the sea bed at it's maximum depth. This means that the thermocline layer reached a maximum depth of 40 m at this location. This was the shallowest location because it is very close to the coast of Sicily. It was the only location where the thermocline extended to the sea floor. As the points approached the northern coast of Malta, the thermocline lower limit reached greater depths. The points along the north transect showed that the lower limit of the thermocline reached a maximum depth of ∼80 m before it disappeared around November 2020 at point 10. It can also be observed that point 10 showed warmer sea water throughout the year compared to the other nine locations in the north. This could have been due to its proximity to the Maltese coast. Another possible cause could have been warmer currents passing nearer to the Maltese Islands.

In the south, the thermocline trend was very similar to that of the north. However, the temperature of the water when the thermocline was not established was slightly warmer than it was in the north. In fact, one can observe the transition in colour from points 11 through 20. This makes sense because, generally, points further south would have a warmer climate, leading to warmer sea temperatures throughout the year.

The MLD was visible above the thermocline layer at all points. In the early developmental stage of the thermocline, the MLD was very shallow, but as the season progressed, it became deeper. The dark red region showed its extent over time. The mixed layer was homogeneous in temperature due to surface mixing. In the fall, this layer remained intact, but the sea temperature became cooler. This can be observed as the region above the thermocline shifted from dark red to light green.

In Chapter 2 of this dissertation, a study conducted by Irmasyithah et al. (2019) was discussed. Their results suggested that productivity is higher when the thermocline layer is closer to the surface. This would imply that in the central Mediterranean Sea, productivity is highest in the months of

July and August. The thermocline was consistently shallower closer to the coast of Sicily. Therefore, productivity would be expected to be higher at the points located in the north, where the sea is not as deep and the thermocline is at its shallowest.

The types of profiles associated with downwelling and upwelling were described in Chapter 2 and examples of them were shown in Figure 2.5 and Figure 2.4. Based on the results showed in the time series heat maps, there were no dates at any points where evidence of downwelling was displayed. This would have been visible in the heat map as a region of colder water above warmer water. There were also no profiles showing characteristics of upwelling. This would have been exemplified as a region of warmer sea water sandwiched between layers of colder water. Though Pinardi et al. (2019) found that the forces that cause upwelling and downwelling are amplified in the MSC, there was no evidence of either from the results of this study.

4.4 Thermocline Thickness

The thickness of the thermocline was plotted over two years from 2020 to 2022. This was done to view the seasonal development of the thermocline layer. The thickness of the thermocline was expected to change over the course of the season. The results can be observed in Figure 4.4.

Figure 4.4a and Figure 4.4b show that, for all points, the trend in thickness was similar. In both regions, the thermocline started out with a thickness between 5 and 10 m in June, and it gradually increased until reaching a maximum of ∼30 m around mid-August, then the thickness decreased until the thermocline disappeared by December. It can be noted that the thickness of the thermocline in the first few months of its establishment was extremely variable. This is shown by the spikes and drops in thickness in the summer months. The cause of these abrupt changes in thickness could have been a result of temporary atmospheric heating. As the air temperatures rises, the sea warms in response, and creates a warm layer of water near the surface. This layer may deepen as more thermal energy is stored within. It is also possible that the thermocline layer was disturbed suddenly due to precipitation, cooler atmospheric temperatures, or increased vertical mixing. Further investigation would be required to address this. After mid-August, the thermocline thickness did not undergo such extreme short term fluctuations. Instead, this marks the time of the year when the thermocline became established, and was not easily disturbed by short term forcing.

Interestingly, the thermocline thickness appeared to follow a somewhat symmetric shape over time. This means that once the maximum thickness has been reached and begins to thin, researchers could predict when the layer would disappear again. This information could be useful for anticipating primary production and migration patterns (Webb, 2023). As certain species are sensitive to temperatures in the larval stage, the onset of the thermocline may be an important factor for their reproductive success (Gardner et al., 2004; Alvarez et al., 2021). Alvarez et al. (2021) studied the effects of the seasonal thermocline on the vertical distribution of bluefin Tuna larvae in the Mediterranean Sea; they found that bluefin tuna larvae are more highly distributed above the thermocline in western Mediterranean Sea. Bluefin tuna fishing and farming is a major economic industry in Malta (Mangion et al., 2018; Said & MacMillan, 2019), and if the vertical distribution of larvae depends on the thermocline layer, understanding its seasonal patterns could potentially be used to increase aquacultural efficiency (Alvarez et al., 2021). Furthermore, a study conducted by Yang et al. (2019) determined that thermocline variability significantly affected the spatial-temporal distribution of bigeye tuna in the Pacific Ocean, therefore, understanding the thermocline layer could have commercial fishing applications which would support the blue economy.

4.5 Salinity and Gradient Profiles

The vertical salinity and gradient profiles proved to differ from the vertical temperature profiles in terms of trends. When the halocline was not expected to be present, the salinity throughout the water column did not change much. When the halocline was detected, the profiles showed slightly higher salinity concentrations near the surface, followed by a layer of less saline water. The same methodology that was used to find the thermocline was applied to locate the halocline. The salinity data downloaded from the CMS catalogue was in units of PSU, therefore the threshold unit was set to PSU/m to plot the gradient profiles. Again, threshold values commonly referenced in the literature were tested at each point along the transects. Based on a visual analysis, the optimal

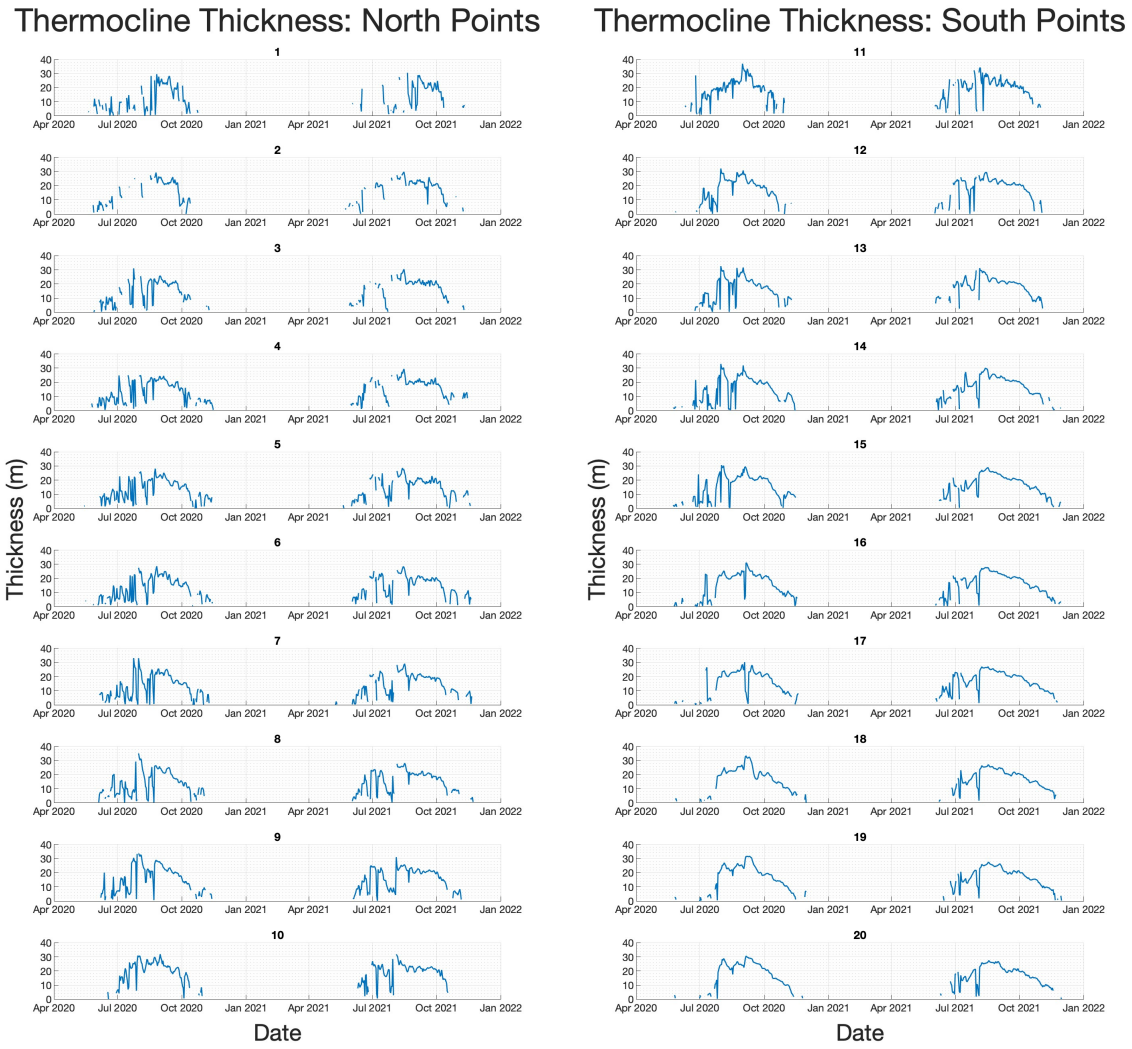

(a) Thermocline thickness: north points

(b) Thermocline thickness: south points

Figure 4.4: Thermocline thickness time series.

threshold was determined to be 0.02 PSU/m. In the literature, this threshold was used to detect weak haloclines (Ueno et al., 2022). Thresholds greater than this value did not detect the halocline in this region. The individual profiles did not provide much information regarding the halocline layer over the long term, hence time series were generated. The results of which will be discussed in the following section.

4.6 Seasonal Variability of the Halocline

Another goal of this project was to identify any seasonal variability of the halocline layer in the regions to the north and to the south of Malta. Based on the results shown in Figure 4.5, the presence of the halocline was less consistent than the thermocline layer was. The threshold chosen to identify the thermocline layer was a value of 0.02 PSU/m. Each crossing is shown on the by coloured markers, where the white and red markers indicate the upper and lower limits of the halocline, respectively. In the literature review, a past paper found that a salinity threshold of 0.02 PSU/m could be used to identify a weak halocline. This threshold was selected because the data used in this study did not show evidence of a strong halocline when different thresholds were tested.

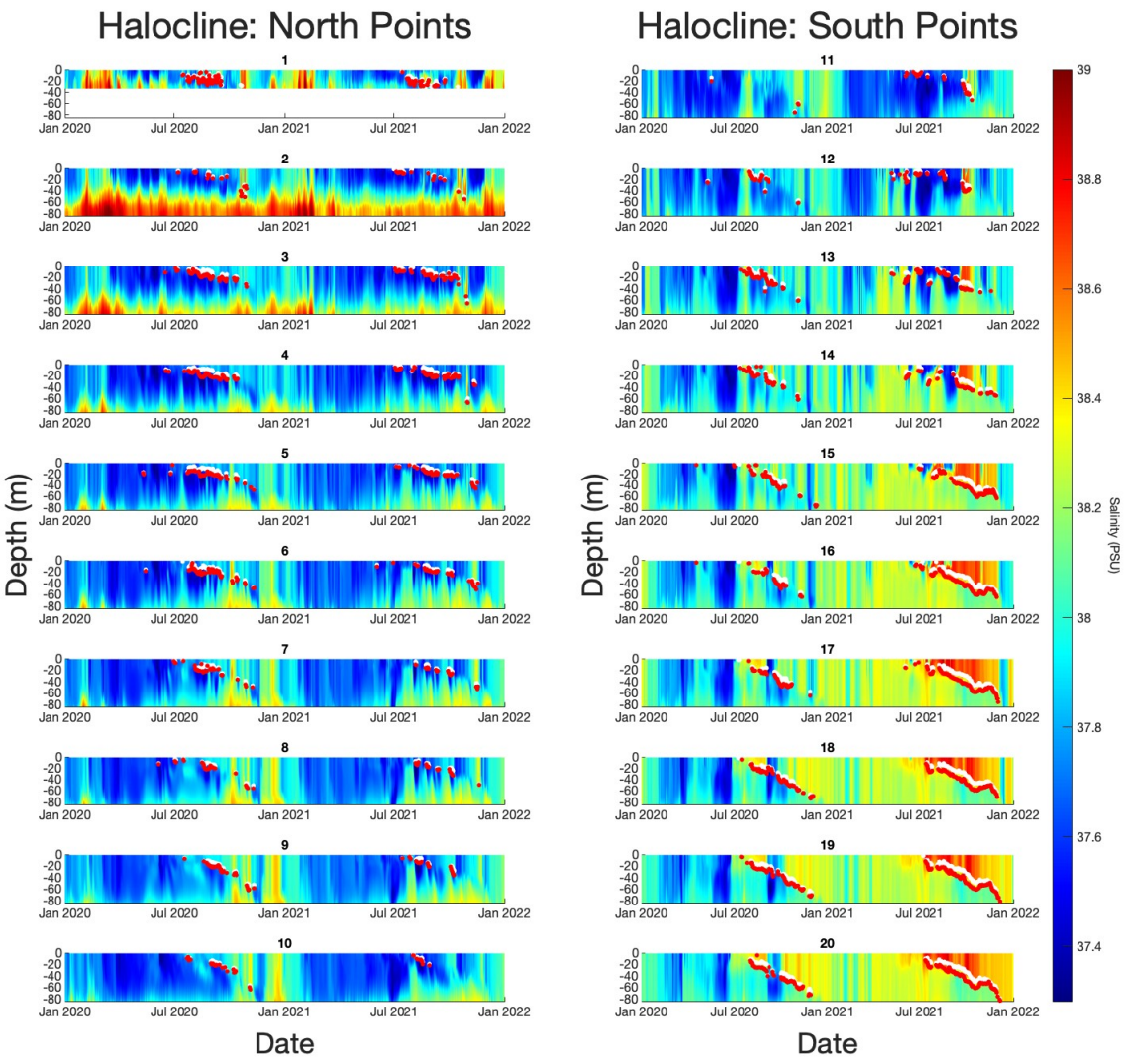

(a) Halocline time series: north points

(b) Halocline time series: south points

Figure 4.5: Time series heat maps showing salinity variation with depth from 2020 to 2022.

With increased sensitivity, the script would be more likely to detect slighter variations in salinity with depth, making the layer boundaries appear more evident in the time series.

Figure 4.5a shows that a weak halocline existed in the north in both seasons in 2020 and 2021. It can be noted that the halocline was present during roughly the same months as the thermocline. It began to form in early summer and disappeared in the winter. This could have been due to increased evaporation of the sea water near the surface, leading to higher salt concentrations.

Point 1 showed little evidence of an established halocline. The white and red markers at this location did not follow a continuous line, but instead were scattered randomly in the summer and fall months. This may have been a result of its proximity to the Sicilian coastline. The salinity at this point could have been impacted by run-off or increased vertical mixing. Point 2 showed a slightly more organized and continuous halocline layer than point 1, but it did not appear to show a very well established layer in either year; there were many dates when there were no detected threshold crossings. Points 3 to 7 have shown more well defined halocline layers that remained intact throughout the summer and fall. This is interesting because these points lie midway between Sicily and Malta. According to modern models of thermohaline circulation in the Mediterranean Sea, the AIS transports fresher sea water east through the MSC (Poulain et al., 2013).

In the south, the halocline layer was only detected on a few days in 2020 at point 11. In 2021 at the same point, there were a few more dates when a halocline was detected, but it did not persist the entire season. The same was true at points 12 and 13. Though the halocline was detected on more days than at point 11, its depth and thickness varied greatly on a short term basis. Points 14 to 20, however, displayed well-established and continuous halocline layers between July and December. It is clear from the plot that there was a difference in the halocline between the two years. The ocean layer above the halocline in 2020 contained a lower concentration of salt than it did in 2021. This could indicate that the halocline layer was stronger in 2021 than in 2020, which could have been due to increased evaporation in 2021 compared to 2020, or perhaps there was more precipitation in 2020. Though these differences existed between the two years, there was a clear pattern of halocline development. Both the trends in layer depth and duration match in 2020 and 2021. What was not consistent was the salinity concentration.

In observing the collection of plots for the points in the south, it is apparent that the overall salinity concentration in PSU increased as the latitude decreased. This is what one would expect as the air temperature would have increased, causing increased evaporation and reduced precipitation as an arid region is approached. It is clear from these plots that the upper 84 m of the Mediterranean Sea at the north points showed consistently lower values of salinity throughout the year compared to the points in the south, with the exception of points 1 and 2 where the sea floor is shallow.

From these results, it can be seen that the points further from the coast developed stronger haloclines. In the shallowest areas that are situated close to the coast of either Malta or Sicily, the seasonal halocline was not well established. It was more distinct midway between Malta and Sicily along the north transect, while it was most distinct in the lower latitudes along the south transect.

4.7 Salinity Variation Between Points

In the previous section, the plots shown in Figure 4.5a and Figure 4.5b only displayed the salinity in the upper 84 m to study the seasonality of the halocline layer. In this section, the entire range of depths will be shown to better understand the salinity concentration distribution.

At the points located in the north, there was an uneven layer of salty water adjacent to the sea floor; this is shown by the dark red portion of the time series. As saltier water is more dense than fresh water, it is logical that this layer existed at the bottom of the MSC. It may have accumulated along the uneven sea floor which would not have experienced as much mixing as the upper layers.

These results agree with larger Mediterranean Sea circulation theories. Specifically, the AIS would be characterized as having low salinity compared to the rest of the Mediterranean Sea and would be found in the upper 0 to 150 m of the sea (Pinardi et al., 2019). The time series for the north and south regions showed lower salt concentrations in the upper 150 m. The profiles do not indicate directionality of the AIS, but it can be assumed that less saline water would have been more likely to originate from the west, and the saline water from the east. As discussed in Chapter 2, the Mediterranean Sea is semi-enclosed, and the main source of incoming low-salt water enters through the Strait of Gibraltar.

It was evident that a permanent halocline exists in the south of Malta. Between 2020 to 2022, this layer extended from approximately 150 m deep to the sea floor. The salinity of the sea water within this layer was between 38.6 and 39 PSU and remained uniform over time. This aligns with the theory that dense, saline sea water that forms in the east Mediterranean, travels back toward the Strait of Gibraltar between Malta and Africa (Pinardi et al., 2019). This sea water would have a higher concentration of salt, causing it to sink to the bottom layer of the ocean. This is what was observed at these points. It can be noted that the points further south showed slightly less saline water below 150 m. This may indicate that the dense saline current is more predominant at points where the salinity concentration was highest beneath the 150 m boundary. However, further research would need to be completed to confirm or deny this.

4.8 Halocline Thickness

The thickness of the halocline was plotted at every point to observe its evolution over time. It was expected that the thickness would change between its onset and disappearance. The plots in Figure 4.7 show the formation of a weak halocline in the north and south. As was discovered in

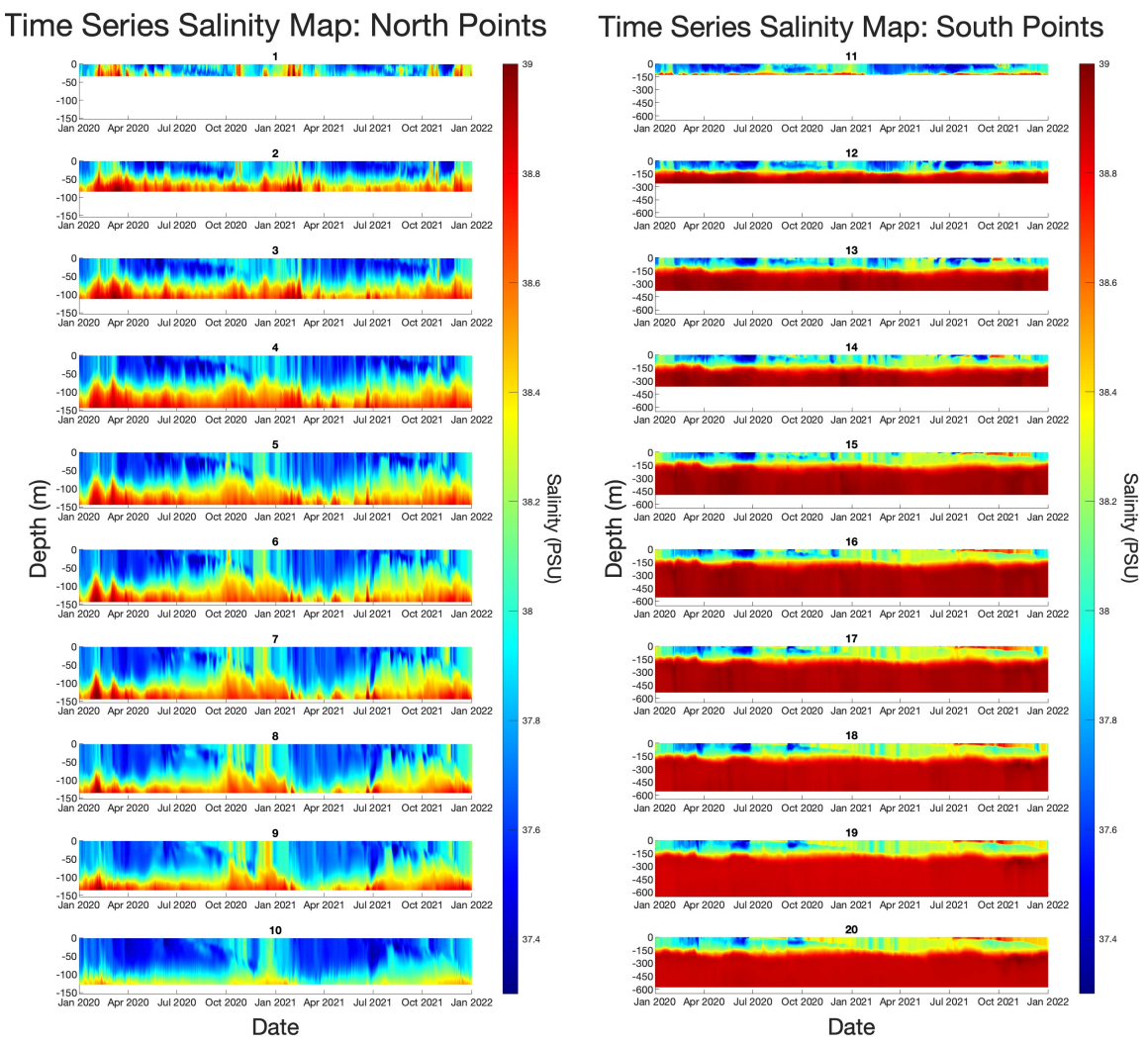

(a) Salinity time series: north points

(b) Salinity time series: south points

Figure 4.6: Time series heat maps showing salinity at all depths.

the previous section, there was scare evidence of a halocline at point 11 in 2020, but there were some dates in 2021 when it was detected at that point. Indeed, points 12 through 14 showed that fragmented halocline layers had formed in the summer and fall months. The layer appeared to be unstable and thin at these points. Compared to the thermocline, the halocline layer lacked continuity in this area. It also demonstrated fluctuations in thickness, as expected.

The cause of an unstable halocline is not clear. What can be said is that there was no sign of halocline formation outside of the period from July to January of each year. The halocline behaviour also varied between years. In the 2020 season, it formed later in the year and was more sporadic than the following year. One possible cause could have been more precipitation in 2020 compared to 2021. This would have led to fresher surface water. Based on these results, it can be concluded that the halocline layer is spatially and temporally variable in the central Mediterranean Sea.

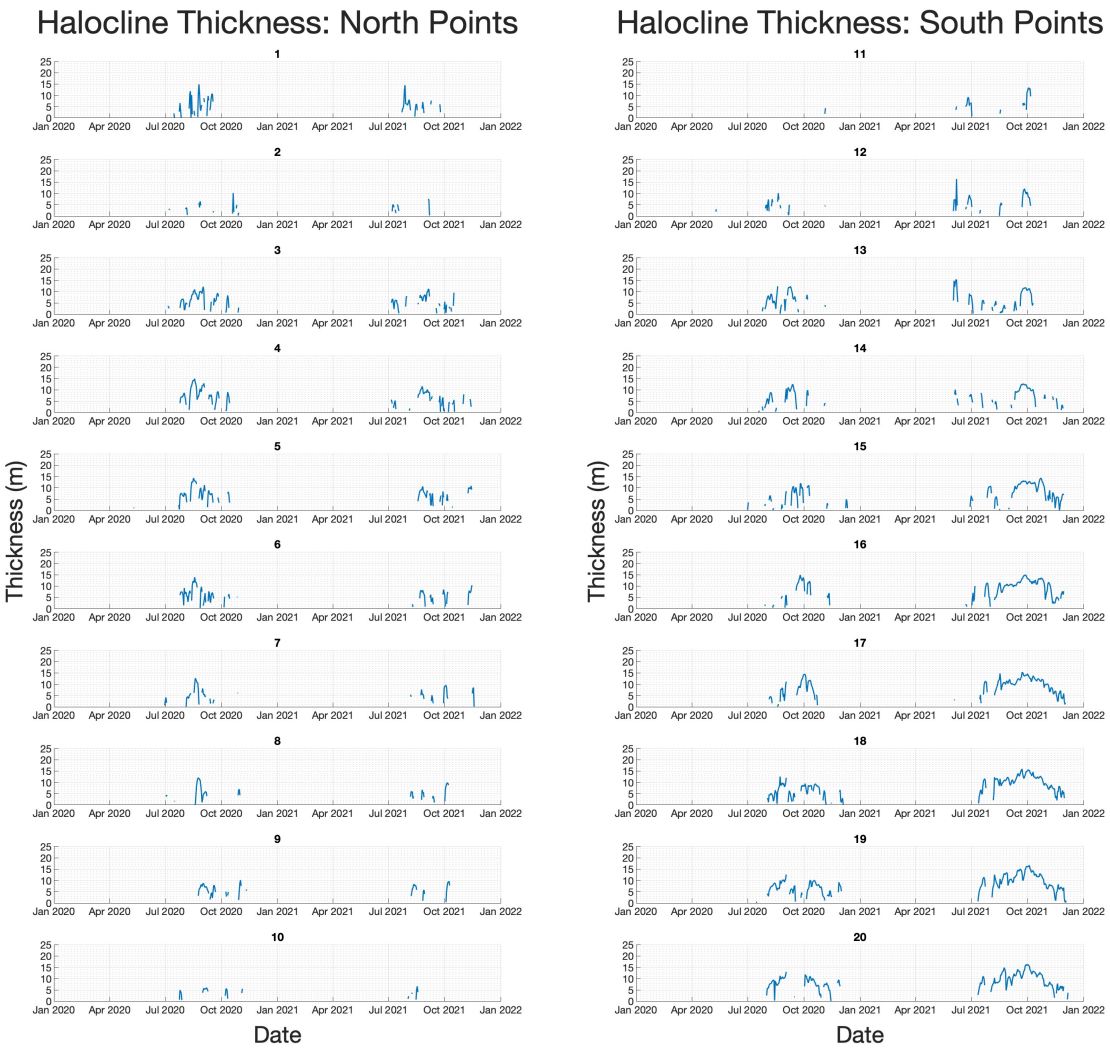

(a) Halocline thickness: north points

(b) Halocline thickness: south points

Figure 4.7: Halocline thickness time series.

4.9 North Versus South

There were many observed differences in the salinity and temperature trends in the north and south. The thermocline was generally shallower in the north. This could have been a result of the depth difference between the points in the north compared to the south. It could have also been due to differences in solar radiation between latitudes. The region between Malta and Sicily lies on a continental shelf. This means the maximum depth in the region does not exceed 200 m. However, the region to the south of Malta reaches much greater depths, with a maximum of around 600 m at point 19. For instance, at point 1, the thermocline extended to the sea floor; it cannot reach depths beyond this limit. Alternatively, the thermocline at the south points was not limited by depth. Furthermore, the temperature of the sea water when the thermocline was not present was fairly consistent throughout the water column. The points located further south showed warmer sea temperatures when the thermocline was not present.

In studying the differences in salinity between the north and south, it became evident that the south featured a more stable permanent halocline than the north. The red portions of the time series heat maps shown in Figures 4.6a and 4.6b rested atop the sea floor. The red areas are those with the highest concentrations of salt. In the south, this red layer was fairly stable and homogeneous. There was a clear boundary where it began. In the north, the red portion was erratic. The boundary where it began was not located at a consistent depth throughout the year. This may have been due to the shallowness of the region, making it more influenced by short term vertical mixing. It is theorized that the denser, more saline water that forms in the east of the Mediterranean Sea is transported towards the Atlantic Ocean. This would mean the supply of salty dense water travels between Malta and Africa, but not much, if any, goes through the MSC. This makes sense because the denser water would be more likely to flow along the bathymetry of the Mediterranean under gravity. This would lead it to tip over continental shelves unless otherwise redirected.

It was hypothesized that the north points would display a less stable seasonal thermocline and halocline than the south points. In terms of salinity, the north region featured a less stable halocline than the south. Moreover, the permanent halocline was found at a less consistent depth in the north than in the south. These observations suggest that the salinity in the north region was less predictable over the short term. The temperature results showed that the thermocline was less stable closer to the coasts of Malta and Sicily. However, the thermocline did not appear to be less stable in the north.

Chapter 5

Conclusions

This chapter includes a summary of the main findings of this study. It will address how each individual aim and its complementary objective was achieved. The hypotheses will be revisited to establish whether they proved to be correct. Following this, the limitations of the project will be discussed and suggestions for improvement in future work will be stated. Lastly, a few final remarks will draw this dissertation to its end.

5.1 Achieved Aims and Objectives

This work can be summarized in the form of its achieved aims and objectives. A collection of four aims and their accompanying objectives were initially proposed. Each of these aims contributed to completing the task of applying CMEMS to monitor seasonal variability of temperature and salinity profiles in the central Mediterranean Sea.

The first aim of this thesis was to detect the thermocline and halocline layers from 2020 to 2022 at every point along the transects to the north and south of Malta. This was achieved by applying the threshold method and completing the objective of generating vertical profiles of temperature and salinity at every point from 2020 to 2022.

The second aim was to observe whether changes in the thermocline and halocline occur in a seasonal cycle. The respective objective completed to achieve this aim was to plot time series heat maps for the temperature and salinity at every point. The time series heat maps showed that the thermocline develops at each point to the north and south of Malta during the summer and fall seasons. They also showed that the halocline developed at the same time as the thermocline, if it formed at all. The halocline layer was weak and unstable compared to the thermocline layer. Despite this, there was a pattern of thermocline and halocline onset and deterioration that repeated seasonally over the two year period. These findings resolved the second aim of the present study.

The third aim was to observe the changes in thicknesses of the thermocline and halocline. The objective of plotting the thickness of each layer was accomplished. The produced plots showed that the thermocline thickness gradually increased until it reached a maximum value and then declined until the layer disappeared. As the thickness over time was symmetric, the thickness of the thermocline after reaching the maximum depth could indicate how much time would remain before the layer would disappear. The plots of halocline thickness showed little consistency between points and years. No discernible pattern was observed other than the general time of year when the halocline was periodically present.

The fourth and final aim was to compare the temperature and salinity characteristics of the north and south regions. It was possible to compare the thermocline and halocline at the points in the north to those in the south based on the respective time series heat maps. The comparison revealed that the seasonal halocline was better established in the south than it was in the north. In the same way, the permanent halocline was more stable in the south where depths exceed 150 m. It was more consistently present in the open ocean compared to coastal waters. Additionally, the thermocline in the north was slightly shallower than it was in the south. By plotting the thickness of the layers as time series, the thermocline thickness was found to be periodically greater in the south than in the north.

In achieving these four aims and their respective objectives, the purpose of this dissertation was met. Nevertheless, it is necessary to address the limitations of this project and consider the possible solutions to be applied in future work in the next section. Additionally, the next few sections will identify any questions that remain unanswered which arose from this study and will provide suggestions for how future work might confront them.

5.2 Critique and Limitations

Though the aims and objectives of this project were achieved, there were limitations that had to be accepted. The first was the lack of validation data. As it was not feasible to collect validation data at each point using a CTD, the CMEMS MSPRP data had to be solely relied upon. The model is well established and has been validated by the CMS, but it is unlikely the validation data was specific to the points studied in this thesis. It is to be expected that a model cannot be 100% accurate, but it was the best option available given the time and resources available for this research.

It is possible that error was introduced by applying the smoothing function in Matlab to the time series. This was done to smooth the colours and remove the lines in the mesh grid, but it would have blurred the adjoining vertical profile data. It is unlikely this would have a significant effect on the bigger picture provided by the graphs, but it should nevertheless be recognized. Additionally, a linear approximation was used to create a continuous dataset from the discretized MSPRP temperature and salinity data. To automate the detection of the thermocline and halocline layers, continuous vertical temperature data was required. This method approximated the temperatures at the depths where data was not provided. The depth data used in this study consisted of 141 unevenly spaced levels. This would mean that any linear approximation errors introduced would not be consistent between depth points. The larger the gap between depth data, the larger the error from the linear approximation. As no in-situ data was collected to compare the results of this study to, it is impossible to calculate the error introduced by this approximation.

It should be noted that the thermocline and halocline detection scripts did not incorporate a reference depth, the function of which is to avoid misidentifying a given layer due to short term fluctuations near the surface. Instead, to avoid this, any profile that did not have either zero or two threshold crossings was not shown on the time series as markers denoting the upper and lower boundaries. It is possible that different results could have been found if a reference depth had been included.

As described in Chapter 2, the threshold method is a widely accepted and applied method of locating the thermocline and halocline layers. However, the literature cited many different threshold values for detecting the thermocline and halocline layers (Irmasyithah et al., 2019; Tubalawony et al., 2024). The lack of justification for threshold selection made it challenging to choose a threshold for use in this study. Steps were taken to select the optimal threshold values by testing a range of values mentioned in the literature to solve this problem. This process was explained in detail in Chapter 3. If a different threshold had been selected, it is possible that the results of this study would have been different. It is also difficult to compare results to studies which used different thresholds.

5.3 Future Work

In future work, it is recommended to collect validation data to ensure the reliability of the model at the study region. This could be done by deploying CTDs at each profile location, or, alternatively, glider or Argo Float data could be acquired.

To address the threshold inconsistency issues, the selection process implemented in this study could be improved and critiqued in succeeding studies. This was beyond the scope of the current research, but it would be interesting to compare the thermocline and halocline results using different threshold values in the Mediterranean Sea. The method used in this study to select the thermocline and halocline thresholds could be improved in future work by conducting a statistical analysis to determine the optimal values.

To expand on the current project, further work could be completed to plot the thermocline and halocline in the years before or after the ones analysed in this thesis. In doing this, it would be possible to observe the yearly variability of these layers. This would help determine if there are any long term temperature or salinity trends. As sea levels and temperatures are anticipated to rise, it could be hypothesized that the salinity would be reduced and the thermocline would exhibit changes over time. These changes would not be visible over the short term.

It would also be interesting to collect weather data over the study region to determine if the lack of layer stability in summer is caused by short term weather events. This could entail comparing air temperature, wind and precipitation data to inter-seasonal thermocline and halocline variations.

A linear interpolation method was chosen to obtain a continuous dataset in this study, but other interpolation methods could be explored. To further reduce error, the scripts could be adapted to include a reference depth to avoid misidentifying the layers. Further research would need to be conducted to determine the ideal reference depth for the study region. In-situ data would be best suited to find this value.

It is worth noting that the scripts produced by this dissertation, located in the Appendix, can be adapted for use in future research. The same scripts may be used to study any variable with depth anywhere in the world for any given time frame, provided the data is available. Though model data was used in this study, the scripts would also function with data collected from CTDs, drifters or other types of instruments. They could be applied to monitor changes over the long or short term.

5.4 Final Remarks

In completing this study on the seasonal variability of the thermocline and halocline layers in the central Mediterranean Sea, it can be concluded that both layers exhibit seasonal patterns. The two layers exist in the summer and fall months, but disappear in the winter and spring. However, the halocline was less consistently present throughout this time. The two layers formed at every point along the transects, which showed that this layer does not exclusively form in coastal waters. In fact, along the south transect, the halocline was more continuously present in the lower latitudes which are located further from the Maltese Islands and continental shelf. At point 11 during the 2020 season, the halocline was only detected on a few days. Overall, the halocline layer appeared to be weaker near Malta and Sicily, and it was less prominent in the north.

The salinity results agree with larger Mediterranean Sea circulation theories. Specifically, the AIS would be characterized as having lower salinity than the rest of the Mediterranean Sea and would be found in the upper 0 to 150 meters of the sea. The time series showed that in the upper 150 meters, the sea showed lower salt concentrations. The profile does not indicate directionality of the AIS, but it can be assumed that less saline water would be more likely to originate from the west.

Overall, temperature and salinity profiles in the central Mediterranean Sea exhibit seasonal changes. In July, the thermocline and halocline layers first begin to appear, and by December they are dissolved. Halocline formation fluctuates along the MSC, but it is more consistently established to the south of Malta. The thermocline is well established in both the north and south, but it shifts to increased depths in the south. There was evidence of a permanent halocline in the north and south of Malta, but possibly due to a lack of depth in the north, was more prominent and stable in the south. This layer is believed to contain the dense, salt-rich water that travels back towards the Atlantic Ocean after forming in the east of the Mediterranean Sea. These findings have demonstrated that the thermocline and halocline develop each year at approximately the same time despite spatial and inter-seasonal variability.

References

Alvarez, I., Rasmuson, L. K., Gerard, T., Laiz-Carrion, R., Hidalgo, M., Lamkin, J. T., Malca, E., Ferra, C., Torres, A. P., Alvarez-Berastegui, D., Alemany, F., Quintanilla, J. M., Martin, M., Rodriguez, J. M., Reglero, P. (2021). Influence of the seasonal thermocline on the vertical distribution of larval fish assemblages associated with Atlantic bluefin tuna spawning grounds. Oceans, 2(1), 64–83. https://doi.org/10.3390/oceans2010004

Andreu-Burillo, I., Holt, J., Proctor, R., Annan, J. D., James, I. D., Prandle, D. (2007). Assimilation of sea surface temperature in the Pol Coastal Ocean Modelling System. Journal of Marine Systems, 65(1–4), 27–40. https://doi.org/10.1016/j.jmarsys.2005.09.017

ARTELIA Group. (n.d.). Wax-coast: Wave extreme value analysis at the Coast. CMEMS. https://marine.copernicus.eu/services/use-cases/wax-coast-wave-extreme-value-analysis-coast

Bonvicini, S. (n.d.). Environmental risk assessment induced by offshore oil spills. CMEMS. https://marine.copernicus.eu/services/use-cases/environmental-risk-assessment-induced-offshore-oil-spills

Chu, P. C., Fan, C. (2023). Global climatological data of ocean thermohaline parameters derived from WOA18. Scientific Data, 10(1). https://doi.org/10.1038/s41597-023-02308-7

Chubarenko, I. P., Demchenko, N. Yu., Esiukova, E. E., Lobchuk, O. I., Karmanov, K. V., Pilipchuk, V. A., Isachenko, I. A., Kuleshov, A. F., Chugaevich, V. Ya., Stepanova, N. B., Krechik, V. A., Bagaev, A. V. (2017). Spring thermocline formation in the coastal zone of the southeastern Baltic Sea based on field data in 2010–2013. Oceanology, 57(5), 632–638. https://doi.org/10.1134/s000143701705006x

Circulation patterns in the Mediterranean Sea. Adapted from The Mediterranean Sea Overturning Circulation by Pinardi et al, 2019, Journal of Physical Oceanography, 49, p. 1715, DOI: 10.1175/JPO-D-18-0254.1. Copyright 2019 American Meteorological Society.

Deidun, A., Gauci, A., Azzopardi, J., Cutajar, D., Farrugia, H., Drago, A. (2016). Which is the best predictor of sea temperature: Satellite, model or data logger values? A case study from the Maltese Islands (Central Mediterranean). Journal of Coastal Research, 75(sp1), 627–631. https://doi.org/10.2112/si75-126.1

EMODnet Digital Bathymetry (DTM 2022). EMODnet product catalogue. (2022, January 31). https://emodnet.ec.europa.eu/geonetwork/srv/eng/catalog.search#/metadata/ff3aff8a-cff1-44a3-a2c8-1910bf109f85

EMODnet. (n.d.). EMODnet Map Viewer. European Marine Observation and Data Network (emodnet). https://emodnet.ec.europa.eu/geoviewer/

Escudier, R., Clementi, E., Omar, M., Cipollone, A., Pistoia, J., Aydogdu, A., Drudi, M., Grandi, A., Lyubartsev, V., Lecci, R., Cretí, S., Masina, S., Coppini, G., Pinardi, N. (2020). Mediterranean Sea Physical Reanalysis (CMEMS MED-Currents) (Version 1) [Data set]. Copernicus Monitoring Environment Marine Service (CMEMS). https://doi.org/10.25423/CMCC/MEDSEA_MULTIYEAR_PHY_006_004_E3R1

Escudier, R., Clementi, E., Cipollone, A., Pistoia, J., Drudi, M., Grandi, A., Lyubartsev, V., Lecci, R., Aydogdu, A., Delrosso, D., Omar, M., Masina, S., Coppini, G., Pinardi, N. (2021). A high resolution reanalysis for the Mediterranean Sea. Frontiers in Earth Science, 9. https://doi.org/10.3389/feart.2021.702285

Escudier, R., Clementi, E., Nigam, T., Aydogdu, A., Fini, E., Pistoia, J., Grandi, A., Miraglio, P. (2022). (issue brief). Mediterranean Sea Production Centre MEDSEA_MULTIYEAR_PHY_006_004. Copernicus Marine Service.

Gardner, C., Maguire, G. B., Williams, H. (2004). Effects of water temperature and thermoclines on larval behaviour and development in the giant crab Pseudocarcinus gigas (Lamarck). Journal of Plankton Research, 26(4), 393–402. https://doi.org/10.1093/plankt/fbh032

Griffies, S. M., Danabasoglu, G., Durack, P. J., Adcroft, A. J., Balaji, V., Böning, C. W., Chassignet, E. P., Curchitser, E., Deshayes, J., Drange, H., Fox-Kemper, B., Gleckler, P. J., Gregory, J. M., Haak, H., Hallberg, R. W., Heimbach, P., Hewitt, H. T., Holland, D. M., Ilyina, T., ... Yeager, S. G. (2016). OMIP contribution to CMIP6: Experimental and diagnostic protocol for the physical component of the Ocean Model Intercomparison Project. Geoscientific Model Development, 9(9), 3231–3296. https://doi.org/10.5194/gmd-9-3231-2016

Haridhi, H. A., Nanda, M., Wilson, C. R., Rizal, S. (2016). Preliminary study of the sea surface temperature (SST) at fishing ground locations based on the net deployment of traditional purse-seine boats in the northern waters of Aceh — a community-based data collection approach. Regional Studies in Marine Science, 8, 114–121. https://doi.org/10.1016/j.rsma.2016.10.002

Haridhi, H. A., Nanda, M., Haditiar, Y., Rizal, S. (2018). Application of rapid appraisals of Fisheries Management System (RAFMS) to identify the seasonal variation of fishing ground locations and its corresponding fish species availability at Aceh waters, Indonesia. Ocean amp; Coastal Management, 154, 46–54. https://doi.org/10.1016/j.ocecoaman.2017.12.030

Hattermann, T. (2018). Antarctic Thermocline Dynamics along a Narrow Shelf with Easterly Winds. Journal of Physical Oceanography, 48(10), 2419-2443. https://doi.org/10.1175/JPO-D-18-0064.1

Horii, T., Ueki, I., Ando, K. (2020). Coastal upwelling events, salinity stratification, and barrier

layer observed along the southwestern coast of Sumatra. Journal of Geophysical Research: Oceans, 125(12). https://doi.org/10.1029/2020jc016287

Irmasyithah, N., Haditiar, Y., Ikhwan, M., Wafdan, R., Setiawan, I., Rizal, S. (2019). Thermocline studies using CMEMS data in the Andaman Sea during October 2017. Earth and Environmental Science, 348(1), 012064. https://doi.org/10.1088/1755-1315/348/1/012064

Janecki, M., Dybowski, D., Rak, D., Dzierzbicka-Glowacka, L. (2022). A New Method for Thermocline and Halocline Depth Determination at Shallow Seas. Journal of Physical Oceanography, 52(9), 2205-2218. https://doi.org/10.1175/JPO-D-22-0008.1

Jean-Baptiste, K. A., Herve, M. A. B., Jeanne, K. M., Andre, T. J. (2017). Seasonal Variation of Thermocline Depth: Consequence on Nutrient Availability in the Ivorian Coastal Zone. European Scientific Journal, ESJ, 13(33), 215. https://doi.org/10.19044/esj.2017.v13n33p215

Kamenkovich, I. V., Sarachik, E. S. (2004). Reducing Errors in Temperature and Salinity in an Ocean Model Forced by Restoring Boundary Conditions. Journal of Physical Oceanography, 34(8), 1856-1869. https://doi.org/10.1175/1520-0485(2004)034<1856:REITAS>2.0.CO;2

Kassis, D., Korres, G. (2021). Recent hydrological status of the Aegean Sea derived from free drifting profilers. Mediterranean Marine Science, 22(2), 347–361. https://doi.org/10.12681/mms.24833

Knauss, J. A., Garfield, N. (2016). The Transfer of Heat across the Ocean Surface. In Introduction to Physical Oceanography: Third Edition (Third, pp. 43–60). essay, Waveband Press.

Liblik, T., Lips, U. (2012). Variability of synoptic-scale quasi-stationary thermohaline stratification patterns in the Gulf of Finland in summer 2009. Ocean Science, 8(4), 603–614. https://doi.org/10.5194/os-8-603-2012

Mangion, M., Borg, J. A., Sanchez-Jerez, P. (2018). Differences in magnitude and spatial extent of impact of tuna farming on benthic macroinvertebrate assemblages. Regional Studies in Marine Science, 18, 197–207. https://doi.org/10.1016/j.rsma.2017.10.008

Map of the Mediterranean. Adapted from The Mediterranean Sea Overturning Circulation by Pinardi et al, 2019, Journal of Physical Oceanography, 49, p. 1700, DOI: 10.1175/JPO-D-18-0254.1. Copyright 2019 American Meteorological Society

Mason, E., Barceló-Llull, B., Sánchez-Román, A., Rodríguez-Tarry, D., Cutolo, E., Delepoulle, A., Ruiz, S., Pascual, A. (2023). Fronts, eddies and mesoscale circulation in the Mediterranean Sea. Oceanography of the Mediterranean Sea, 263–287. https://doi.org/10.1016/b978-0-12-823692-5.00003-0

Mediterranean Sea Physics Reanalysis Product. E.U. Copernicus Marine Service Information

(CMEMS). Marine Data Store (MDS). https://doi.org/10.25423/CMCC/MEDSEA_MULTIYEAR_PHY_006_004_E3R1

Nigam, T., Escudier, R., Pistoia, J., Aydogdu, A., Omar, M., Clementi, E., Cipollone, A., Drudi, M., Grandi, A., Mariani, A., Lyubartsev, V., Lecci, R., Cretí, S., Masina, S., Coppini, G., Pinardi, N. (2021). Mediterranean Sea Physical Reanalysis INTERIM (CMEMS MED-Currents, E3R1i system) (Version 1) [Data set]. Copernicus Monitoring Environment Marine Service (CMEMS). https://doi.org/10.25423/CMCC/MEDSEA_MULTIYEAR_PHY_006_004_E3R1I

Ocean Circulation - ocean climate platform. Ocean Climate Platform - A healthy ocean, a protected climate. (2020, January 30). https://ocean-climate.org/en/awareness/ocean-circulation/

Pinardi, N., Cessi, P., Borile, F., Wolfe, C. L. (2019). The Mediterranean Sea Overturning Circulation. Journal of Physical Oceanography, 49(7), 1699–1721. https://doi.org/10.1175/jpo-d-18-0254.1

Pinardi, N., Estournel, C., Cessi, P., Escudier, R., Lyubartsev, V. (2023). Dense and deep water formation processes and Mediterranean overturning circulation. Oceanography of the Mediterranean Sea, 209–261. https://doi.org/10.1016/b978-0-12-823692-5.00009-1

Poulain, P.-M., Bussani, A., Gerin, R., Jungwirth, R., Mauri, E., Menna, M., Notarstefano, G. (2013). Mediterranean surface currents measured with drifters: From basin to subinertial scales. Oceanography, 26(1), 38–47. https://doi.org/10.5670/oceanog.2013.03

Poulos, S. E. (2020). The Mediterranean and Black Sea Marine system: An overview of its physico-geographic and oceanographic characteristics. Earth-Science Reviews, 200, 103004. https://doi.org/10.1016/j.earscirev.2019.103004

Rivetti, I., Boero, F., Fraschetti, S., Zambianchi, E., Lionello, P. (2017). Anomalies of the upper water column in the Mediterranean Sea. Global and Planetary Change, 151, 68–79. https://doi.org/10.1016/j.gloplacha.2016.03.001

Romanou, A., Tselioudis, G., Zerefos, C. S., Clayson, C., Curry, J. A., Andersson, A. (2010). Evaporation–Precipitation Variability over the Mediterranean and the Black Seas from Satellite and Reanalysis Estimates. Journal of Climate, 23(19), 5268-5287. https://doi.org/10.1175/2010JCLI3525.1

Said, A., MacMillan, D. (2019). 're-grabbing' marine resources: A blue degrowth agenda for the resurgence of small-scale fisheries in Malta. Sustainability Science, 15(1), 91–102. https://doi.org/10.1007/s11625-019-00769-7

Schroeder, K., Chiggiato, J. (2023). Oceanography of the Mediterranean Sea: An introductory guide. Elsevier.

Slišković, M., Gudelj, A., Piria, M. (2024). A Systematic Analysis of the Mediterranean Sea (IHO Sea Area) in the WRiMS Database. Diversity, 16(7), 358. https://doi.org/10.3390/d16070358

Stewart, R. H. (2008). Introduction to physical oceanography. A M University.

Treguier, A. M., de Boyer Montégut, C., Bozec, A., Chassignet, E. P., Fox-Kemper, B., McC. Hogg, A., Iovino, D., Kiss, A. E., Le Sommer, J., Li, Y., Lin, P., Lique, C., Liu, H., Serazin, G., Sidorenko, D., Wang, Q., Xu, X., Yeager, S. (2023). The mixed-layer depth in the Ocean Model Intercomparison Project (OMIP): Impact of resolving mesoscale eddies. Geoscientific Model Development, 16(13), 3849–3872. https://doi.org/10.5194/gmd-16-3849-2023

Tubalawony, S., Hukubun, R. D., Kalay, D. E. (2024). The Seasonal Variations of the Thermocline in the Banda Sea and its Water Mass Characteristics. Jurnal Penelitian Pendidikan IPA, 10(SpecialIssue), 534–545. https://doi.org/10.29303/jppipa.v10iSpecialIssue.9071

Ueno, H., Oda, M., Yasui, K., Dobashi, R., Mitsudera, H. (2022). Global distribution and interannual variation in the winter halocline. Journal of Physical Oceanography, 52(4), 665–676. https://doi.org/10.1175/jpo-d-21-0056.1

Webb, P. (2023). Patterns of Primary Production. In Introduction to Oceanography. essay, Pressbooks.

What is a thermocline?. NOAA's National Ocean Service. (n.d.). https://oceanservice.noaa.gov/facts/thermocline.html

Yang, S., Zhang, B., Zhang, H., Zhang, S., Fan, X., Hua, C., Fan, W. (2019). Bigeye tuna fishing ground in relation to thermocline in the Western and Central Pacific Ocean using Argo data. Indian Journal of Geo Marine Sciences, 48(4), 444–451.

Zhang, H. (2023). Modulation of Upper Ocean Vertical Temperature Structure and Heat Content by a Fast-Moving Tropical Cyclone. Journal of Physical Oceanography, 53(2), 493-508. https://doi.org/10.1175/JPO-D-22-0132.1

Appendix A

Matlab Scripts

The complete scripts written in Matlab to complete this project are found below.

A.1 Plotting the Vertical Temperature and Gradient Profiles

```
temp = ncread('north_temp_data.nc','thetao',[22 12 1 15],[1 1 Inf
    1]); %[startlon startlat startdepth startday], [numlon numlat
    numdepth numday] reads the temperature data on a given date at
    all depths at coordinate values lon = 22 and lat = 12 e.g.(
    January 15th 2020 at point 7)
depth = ncread("north_temp_data.nc", 'depth');   %reads the depth
    data

t = squeeze(temp);   %format data
d = (-1)*depth;    %assign negative depth values (more intuitive)

%finding the change in depth and temperature between each data point

dt = t(1:end-1)-t(2:end);  %change in temperature (difference
    between tempwrature values)
dx = d(1:end-1)-d(2:end);  %change in depth (differece between depth
     points)
dtdx = dt./dx;  %change in temperature per unit depth (gradient)

%plotting depth against dt/dx to locate threshold crossings
x0 = 0.2;  %value of the threshold (degC/m)
figure;
plot(dtdx, d(1:end-1), 'X-','LineWidth',2);  %plots the temperature
    gradient against depth
xlabel('dt/dx (degC/m)')
ylabel('Depth (m)')
yticks(-140:10:0)  %add tick marks on the y axis
ylim([-140 0])
xlim([-0.1 0.4])  %set x and y limits of the graph
title('Temperature Gradient Profile: Point #7 on January 15th, 2020'
    )
grid on
grid minor
hold on;
xline(x0,'--r', 'LineWidth',2);  %plot the threshold value as a line

x = dtdx;
y = d(1:end-1);

plot(x,y)  %reassign variable names for counting later
```

```
%plotting the temperature profile

figure;
plot(t, d, 'X-', 'LineWidth',2)  %plots the temperature profile
xlabel('Temperature (degC)')
ylabel('Depth (m)')
yticks(-140:10:0)
ylim([-140 0])
title('Vertical Temperature Profile: Point #7 on January 15th, 2020'
   )
xlim([14 30.5])
grid on
grid minor
hold on;

%counting the number of times the threshold is crossed

crossneg=0; crosspos=0;
for i=1:length(y)
    if x(i)<=x0 && x(i+1)>=x0  %crosses when depth is decreasing (
       neg slope)
        crossneg=crossneg+1;  %add a count each time its crossed
        ythresneg(crossneg)=y(i);  %find y index of value before the
            threshold is crossed
        ythresneg2(crossneg)=y(i+1);  %find y index of neighbour
           value
        m = (y(i)-y(i+1))./(x(i)-x(i+1));  %calculate slope
        y0 = m*(x0 - x(i)) + y(i)  %calculate exact depth when
           threshold is crossed
        yline(y0, '--r', 'LineWidth',2);  %plot thermocline on temp
           profile
    elseif x(i)>=x0 && x(i+1)<=x0  %crosses when decreasing in
       opposite direction (positive slope)
        crosspos=crosspos+1;  %add a count each time its crossed
        ythrespos(crosspos)=y(i);  %find y index of value before the
            threshold is crossed
        ythrespos2(crosspos)=y(i+1);  %find y index of neighbour
           value
        m2 = (y(i)-y(i+1))./(x(i)-x(i+1));  %calculate slope
        y02 = m2*(x0 - x(i)) + y(i)  %calculate exact depth when
           threshold is crossed
        yline(y02, '--r','LineWidth',2);  %plot thermocline on temp
           profile
    end
end
counts = crossneg + crosspos;  %calculate total number of times
   threshold is crossed
fprintf('Found %d counts',counts);  %print the value
```

A.2 Mapping Points

```
figure   %create a figure to show the locations of the points along
   the transects
geobasemap topographic   %add a basemap
```

```
for n = 24:-2:6   %create a loop to add all the points along the
    north transect (latitude values 24 to 6, skipping every number
    between)
     lat = ncread('north_temp_data.nc','latitude', n, 1);   %plot the
          points for each latitude
     lon = ncread('north_temp_data.nc','longitude', 22, 1);   %the
        longitude remains the same for every point

        %add a marker for every point
     labels = {num2str(11 - (n./2 - 2))};   %giving them labels from
        1 to 10
     text(lat,lon,labels,'VerticalAlignment','bottom','
        HorizontalAlignment','right')   %formatting
     hold on
     geoplot(lat,lon,"om",MarkerFaceColor="magenta")   %plot the
        markers

end

hold on

for n = 81:-2:63   %now add the points along the southern transect
     lat = ncread('south_temp_data.nc','latitude', n, 1);   %values
        of n are used to find each latitude
     lon = ncread('south_temp_data.nc','longitude', 14, 1);   %the
        longitude remains the same
     labels = {num2str( 31-(((((n-39)/2)-2))+1) )};   %label these 11
          to 20
     text(lat,lon,labels,'VerticalAlignment','bottom','
        HorizontalAlignment','right')
     hold on    %add a marker for every point
     geoplot(lat,lon,"om",MarkerFaceColor="blue")   %show these
        points on the map in a different color
end

title("Points Along Transects to the North and South of Malta")  %
    add a title for the map
geolimits([34.75 37],[14 15])   %set the geographical limits of the
    map
```

A.3 Time Series Heat Map

```
%general information

depth = ncread("north_temp_data.nc", 'depth');   %read the depth
    data
d = (-1)*depth;   %convert the values to negative

StartDate = '01-jan-2020';   %define the start date of the dataset
EndDate = '01-jan-2022';   %define the end date of the dataset
DateVec = datetime(StartDate);   %use datetime to convert numerical
    values to dates
EndDateVec = datetime(EndDate);
dates = DateVec:days(1):EndDateVec;
```

```
%plotting north points
figure();
    t = tiledlayout('vertical');
    title(t, "Time Series Heat Map: North Points", 'FontSize', 25)
         %add a label for all the tiles
    xlabel(t,'Date', 'FontSize', 18)   %make axis labels for every
       tile
    ylabel(t,'Depth (m)', 'FontSize', 18)

for k = 24:-2:6

    for thresholds = 0.2   %0.1:0.05:0.4    %repeat the calculations
        for 4 different threshold values

        temp0 = ncread('north_temp_data.nc','thetao',[22 k 1 1],[1 1
            Inf Inf]);  %read the temperature data for a particular
           coordinate
        temp0 = squeeze(temp0);   %squeeze the data
        [~,Depth_Grid] = meshgrid(dates,d);   %create a grid the
           size of the dates x depths
        profiles0 = temp0;   %store the temperature data
        depth0 = Depth_Grid;

        thermocline0 = [];   %create an empty array
        for day=1:1:length(depth0)
            thermodata=finddepths(profiles0(:,day),depth0(:,day),
               thresholds);  %apply function for each point and each
                threshold
            thermocline0=[thermocline0; thermodata];   %store the
               data in the empty array
        end

        ax = nexttile;   %in the loop, keep adding plots for
           different threshold values

        hold on
        [Time_Grid,Depth_Grid] = meshgrid(dates,d);   %create an
           empty meshgrid the size of the dates x depths
        pcolor(dates,Depth_Grid,temp0);   %use pcolor to visualize
           the temperature/salinity changes
        ylim([-84.7400 0])   %define the depth limit to be shown in
           the meshgrid

        title(num2str(11 - (k./2 - 2)))   %number each tile in the
           tiledlayout according to point #
        colormap("jet");   %choose an intuitive color range
        shading interp    %smooth the meshgrid
        view(2)
        ax = scatter(dates, thermocline0(:,2:3), 45, '.');   %add
           the crossing markers to the meshgrid (only the dates
           where exactly two crossings occurred)

    end
    hold off

%optional code to save plot to a folder:
    %set(gcf, 'Units', 'Normalized', 'OuterPosition', [0 0 1 1]);
```

```
    %plots = ['north_temp_testing_threshold_vals',num2str(k),'.jpg']
        % plot names
    %saveas(gcf,plots,'jpg') % gcf to save the whole figure window
end
cb = colorbar;   %add a universal color bar
clim([14 30.5])   %set the temperature/salinity limits
cb.Layout.Tile = 'east';
ylabel(cb, 'Temp (degC)','FontSize',18,'Rotation',270);   %format
   the color bar


%plotting south points

depth = ncread("south_temp_data.nc", 'depth');
d = (-1)*depth;

figure();
t = tiledlayout('vertical');
title(t, "Time Series Heat Map: South Points", 'FontSize', 25)   %
   add a label for all the tiles
xlabel(t,'Date', 'FontSize', 18)
                                                                %
   make axis labels for every tile
ylabel(t,'Depth (m)', 'FontSize', 18)

for k = 81:-2:63

    for thresholds =  0.2  %0.1:0.05:0.4
                                                        %repeat the
        calculations for 4 different threshold values

        temp0 = ncread('south_temp_data.nc','thetao',[14 k 1 1],[1 1
            Inf Inf]);   %read the temperature data for a particular
            coordinate
        temp0 = squeeze(temp0);   %squeeze the data
        [~,Depth_Grid] = meshgrid(dates,d);   %create a grid the
           size of the dates x depths
        profiles0 = temp0;   %store the temperature data
        depth0 = Depth_Grid;

        thermocline0 = [];
        for day=1:1:length(depth0)
            thermodata=finddepths(profiles0(:,day),depth0(:,day),
               thresholds);
            thermocline0=[thermocline0; thermodata];
        end

        ax = nexttile;   %in the loop, keep adding plots for
           different threshold values
        hold on
        [Time_Grid,Depth_Grid] = meshgrid(dates,d);
        pcolor(dates,Depth_Grid,temp0);
        ylim([-84.7400 0])
        yticks([-80 -60 -40 -20 0])
        title(num2str( 31-(((((k-39)/2)-2))+1)))   %add the value of
            the threshold to the title to identify each plot
        colormap("jet");
```

```
        shading interp
        view(2)
        ax = scatter(dates, thermocline0(:,2:5), 40, '.');
        %legend(ax, '1st', '2nd')  %can add a legend
    end
    hold off

%optional code for saving the plot to a folder:
    %set(gcf, 'Units', 'Normalized', 'OuterPosition', [0 0 1 1]);
    %plots = ['south_timeseries',num2str(k),'.jpg'] % plot names
    %saveas(gcf,plots,'jpg') % gcf to save the whole figure window
end
    cb = colorbar;
    cb.Layout.Tile = 'east';
    clim([14 30.5])
    ylabel(cb, 'Temp (degC)','FontSize',18,'Rotation',270);
```

A.4 Finding the Depths of each Threshold Crossing

```
function [thermocline] = finddepths(tprofile,tdepths,threshold)
%for any given Temp profile and given threshold, find the depths
   based on threshold

t=tprofile;
z=tdepths;
dtdz0=threshold; %threshold value of dtdz (degC/m)
zdepths=[NaN, NaN, NaN, NaN, NaN, NaN];  %create an empty matrix
   filled with NaN

%step1: find gradient
dt = t(1:end-1)-t(2:end);  %change in temperature (difference
   between temperature values)
dz = z(1:end-1)-z(2:end);  %change in depth (difference between
   depth points)
dtdz = dt./dz;  %change in temperature per unit depth
for i=1:1:length(z)-1
    zgrad(i) = (z(i)+z(i+1))/2;
end
%to plot gradients: yaxis=zgrad,xaxis=dtdz .... plot(dtdz,zgrad,'o-r
   ');

%step2: find crossings
ncross=0;
for i=1:length(dtdz)
    if ( dtdz(i)<=dtdz0 && dtdz(i+1)>=dtdz0 ) || ( dtdz(i)>=dtdz0 &&
        dtdz(i+1)<=dtdz0 )
                                                                %
       crosses when depth is decreasing (neg slope)
        m = (zgrad(i)-zgrad(i+1))/(dtdz(i)-dtdz(i+1));  %calculate
           slope
        c = zgrad(i+1) - (m*dtdz(i+1));
        z0 = (m*(dtdz0)) + c;  %calculate exact depth when threshold
            is crossed
        ncross=ncross+1;  %add a count each time its crossed
        zdepths(ncross)=z0;
```

```
    end
end
thermocline=[ncross, zdepths]; %ideally be a vector size 1r 5c
```

A.5 Bar Graphs to Test Thresholds

```
%bar graphs to determine the optimal threshold
depth = ncread("north_temp_data.nc", 'depth');
d = (-1)*depth;

StartDate = '01-jan-2020';
EndDate = '01-jan-2022';
DateVec = datetime(StartDate);
EndDateVec = datetime(EndDate);
dates = DateVec:days(1):EndDateVec;

for k = 24:-2:6  %repeat for every point
    figure(k);  %produce a new figure for each point

    t = tiledlayout('vertical');
    title(t, "Testing thresholds: North Points", 'fontSize', 19)  %
       add a label for all the tiles
    xlabel(t,'Crossings', 'fontSize', 18)  %make axis labels for
       every tile
    ylabel(t,'Counts', 'fontSize', 18)

    for thresholds = 0.1:0.05:0.4   %repeat the calculations for 4
       different threshold values (in this case for temperature)

        temp0 = ncread('north_temp_data.nc','thetao',[22 k 1 1],[1 1
            Inf Inf]);  %read the temperature data for a particular
           coordinate
        temp0 = squeeze(temp0);  %squeeze the data
        [~,Depth_Grid] = meshgrid(dates,d);   %create a grid the
           size of the dates x depths
        profiles0 = temp0;  %store the temperature data
        depth0 = Depth_Grid;

        thermocline0 = [];
        for day=1:1:length(depth0)
            thermodata=finddepths(profiles0(:,day),depth0(:,day),
               thresholds);
            thermocline0=[thermocline0; thermodata];
        end

        ax = nexttile;   %in the loop, keep adding plots for
           different threshold values
        hold on
        title(thresholds)
        thresholddata = thermocline0(:,1);
        ctrs = [min(thresholddata):max(thresholddata)];
        cnt = hist(thresholddata,ctrs);
        out = [ctrs; cnt];
        xlim([-0.5 7])
        ylim([0 750])
```

```
        yticks(0:150:750)
        bar(ctrs, cnt, 'r')
        grid on
        grid minor

    end

end

%south points

depth = ncread("south_temp_data.nc", 'depth');
d = (-1)*depth;

for k = 81:-2:63
    figure(k);

    t = tiledlayout('vertical');
    title(t, "Testing Thresholds: South Points")  %add a label for
       all the tiles
    xlabel(t,'Crossings')  %make axis labels for every tile
    ylabel(t,'Counts')

    for thresholds = 0.1:0.05:0.4   %repeat the calculations for 4
       different threshold values

        temp0 = ncread('south_temp_data.nc','thetao',[14 k 1 1],[1 1
            Inf Inf]);  %read the temperature data for a particular
           coordinate
        temp0 = squeeze(temp0);   %squeeze the data
        [~,Depth_Grid] = meshgrid(dates,d);   %create a grid the
           size of the dates x depths
        profiles0 = temp0;   %store the temperature data
        depth0 = Depth_Grid;

        thermocline0 = [];
        for day=1:1:length(depth0)
            thermodata=finddepths(profiles0(:,day),depth0(:,day),
               thresholds);
            thermocline0=[thermocline0; thermodata];
        end

        ax = nexttile;  %in the loop, keep adding plots for
           different threshold values
        hold on
        title(thresholds)
        thresholddata = thermocline0(:,1);
        ctrs = [min(thresholddata):max(thresholddata)];
        cnt = hist(thresholddata,ctrs);
        out = [ctrs; cnt];
        xlim([-0.5 7])
        ylim([0 600])
        bar(ctrs, cnt, 'r')
        grid

    end
```

```
end
```

A.6 Plotting Layer Thickness

```
%plotting the thickness of the thermocline

%north points
depth = ncread("north_temp_data.nc", 'depth');
d = (-1)*depth;

StartDate = '01-jan-2020';
EndDate = '01-jan-2022';
DateVec = datetime(StartDate);
EndDateVec = datetime(EndDate);
dates = DateVec:days(1):EndDateVec;

figure();
    t = tiledlayout('vertical');
    title(t, "Thermocline Thickness: North Points", "fontSize", 25)
        %add a label for all the tiles
    xlabel(t,'Date', "fontSize", 18)   %make axis labels for every
       tile
    ylabel(t,'Thickness (m)', "fontSize", 18)

for k = 24:-2:6

    thresholds = 0.2;

    temp0 = ncread('north_temp_data.nc','thetao',[22 k 1 1],[1 1 Inf
        Inf]);  %read the temperature data for a particular
       coordinate
    temp0 = squeeze(temp0);  %squeeze the data
    [~,Depth_Grid] = meshgrid(dates,d);  %create a grid the size of
       the dates x depths
    profiles0 = temp0;  %store the temperature data
    depth0 = Depth_Grid;

    thermocline0 = [];
    for day=1:1:length(depth0)
        thermodata=finddepths(profiles0(:,day),depth0(:,day),
           thresholds);
        thermocline0=[thermocline0; thermodata];
    end

    ax = nexttile;
    hold on

    thermocline0(thermocline0(:,1)~=2) = 0;
    plot(dates, thermocline0(:,2)-thermocline0(:,3), 'LineWidth'
       ,1.5)
    grid on
    grid minor
    ylim([0 40])
    yticks([0 10 20 30 40])
    title(num2str(11 - (k./2 - 2)))
```

```
end

%south points

depth = ncread("south_temp_data.nc", 'depth');
d = (-1)*depth;

t = tiledlayout('vertical');
title(t, "Thermocline Thickness: South Points", 'fontsize', 25) %add
    a label for all the tiles
xlabel(t,'Date', 'fontsize', 18)
                                                                %
   make axis labels for every tile
ylabel(t,'Thickness (m)', 'fontsize', 18)

for k = 81:-2:63

    thresholds = 0.2;

    temp0 = ncread('south_temp_data.nc','thetao',[14 k 1 1],[1 1 Inf
        Inf]);  %read the temperature data for a particular
       coordinate
    temp0 = squeeze(temp0);  %squeeze the data
    [~,Depth_Grid] = meshgrid(dates,d);  %create a grid the size of
       the dates x depths
    profiles0 = temp0;  %store the temperature data
    depth0 = Depth_Grid;

    thermocline0 = [];
    for day=1:1:length(depth0)
        thermodata=finddepths(profiles0(:,day),depth0(:,day),
           thresholds);
        thermocline0=[thermocline0; thermodata];
    end

    ax = nexttile;
    hold on

    thermocline0(thermocline0(:,1)~=2) = 0;
    plot(dates, thermocline0(:,2)-thermocline0(:,3), 'LineWidth'
       ,1.5)
    title(num2str( 31-(((((k-39)/2)-2))+1)))
    ylim([0 40])
    yticks([0 10 20 30 40])
    grid on
    grid minor

end
```

Appendix B

Depth Intervals

Depth Level	Depth (m)	Depth Level	Depth (m)	Depth Level	Depth (m)
1	0	48	348.75195	95	1889.6127
2	1.0182366	49	364.82196	96	1944.9471
3	3.1657474	50	381.41544	97	2001.4166
4	5.4649634	51	398.54471	98	2059.0291
5	7.9203773	52	416.22232	99	2117.7925
6	10.536604	53	434.46106	100	2177.7141
7	13.318384	54	453.27377	101	2238.8003
8	16.270586	55	472.67349	102	2301.0576
9	19.398211	56	492.67346	103	2364.4917
10	22.706392	57	513.28699	104	2429.1077
11	26.200399	58	534.52759	105	2494.9102
12	29.885643	59	556.40887	106	2561.9031
13	33.767673	60	578.94458	107	2630.0898
14	37.852192	61	602.14862	108	2699.4736
15	42.145039	62	626.03491	109	2770.0566
16	46.65221	63	650.61755	110	2841.8408
17	51.37986	64	675.91071	111	2914.8269
18	56.334286	65	701.92865	112	2989.0159
19	61.521957	66	728.68561	113	3064.4075
20	66.949493	67	756.19604	114	3141.0015
21	72.623688	68	784.4743	115	3218.7961
22	78.551498	69	813.53485	116	3297.7903
23	84.740044	70	843.39215	117	3377.9814
24	91.196632	71	874.06067	118	3459.3662
25	97.928726	72	905.55481	119	3541.9419
26	104.94398	73	937.8891	120	3625.7039
27	112.25021	74	971.07788	121	3710.6475
28	119.85543	75	1005.1355	122	3796.7681
29	127.76784	76	1040.0763	123	3884.0596
30	135.9958	77	1075.9143	124	3972.5161
31	144.5479	78	1112.6637	125	4062.1304
32	153.43285	79	1150.3384	126	4152.896
33	162.65962	80	1188.9521	127	4244.8042
34	172.23735	81	1228.5188	128	4337.8477
35	182.17535	82	1269.0518	129	4432.0176
36	192.48314	83	1310.5642	130	4527.3042
37	203.17044	84	1353.0693	131	4623.6987
38	214.24716	85	1396.58	132	4721.1914
39	225.7234	86	1441.1086	133	4819.771
40	237.60947	87	1486.6678	134	4919.4272
41	249.91585	88	1533.2694	135	5020.1494
42	262.65323	89	1580.9252	136	5121.9258
43	275.83252	90	1629.6466	137	5224.7446
44	289.46478	91	1679.4448	138	5328.5938
45	303.56131	92	1730.3303	139	5433.4609
46	318.13354	93	1782.3136	140	5539.3335
47	333.19315	94	1835.4045	141	5646.1992

Table B.1: Note. This table was created using vertical depth data downloaded from the Copernicus Marine Service Mediterranean Sea Physics Reanalysis Product (www.marine.copernicus.eu).